



Minnesota State University, Mankato
Cornerstone: A Collection of Scholarly
and Creative Works for Minnesota
State University, Mankato

All Theses, Dissertations, and Other Capstone
Projects

Theses, Dissertations, and Other Capstone
Projects

2019

The Concept of Substrate Integrated Circularly Polarized Horn Antennas

Venkata Naga Kalyan Ram Akunuru
Minnesota State University, Mankato

Follow this and additional works at: <https://cornerstone.lib.mnsu.edu/etds>



Part of the [Electrical and Electronics Commons](#), and the [VLSI and Circuits, Embedded and Hardware Systems Commons](#)

Recommended Citation

Акunuru, V. N. K. R. (2019). The concept of substrate integrated circularly polarized horn antennas [Master's thesis, Minnesota State University, Mankato]. Cornerstone: A Collection of Scholarly and Creative Works for Minnesota State University, Mankato. <https://cornerstone.lib.mnsu.edu/etds/915/>

This Thesis is brought to you for free and open access by the Theses, Dissertations, and Other Capstone Projects at Cornerstone: A Collection of Scholarly and Creative Works for Minnesota State University, Mankato. It has been accepted for inclusion in All Theses, Dissertations, and Other Capstone Projects by an authorized administrator of Cornerstone: A Collection of Scholarly and Creative Works for Minnesota State University, Mankato.

**The concept of Substrate Integrated Circularly Polarized Horn
Antennas**

By

Venkata Naga Kalyan Ram Akunuru

A Thesis Submitted in Partial Fulfillment of the
Requirements for the Degree of
Master of Science

In

Electrical and Computer Engineering Technology

Minnesota State University, Mankato

Mankato, Minnesota

05/2019

Date: **04/12/2019**

Title: **The concept of Substrate Integrated Circularly Polarized Horn Antennas**

Student's Name: **Venkata Naga Kalyan Ram Akunuru**

This thesis has been examined and approved by the following members of the student's committee.

Advisor

Committee Member

Committee Member

Declaration of Authorship

I, Venkata Naga Kalyan Ram Akunuru, declare that this thesis titled, “The concept of novel Substrate Integrated Circularly Polarized Horn Antennas” and the work presented in it are my own. I confirm that:

- This work was done wholly or mainly while in candidature for a research degree at this University.
- Where any part of this thesis has previously been submitted for a degree or any other qualification at this University or any other institution, this has been clearly stated.
- Where I have consulted the published work of others, this is always clearly attributed.
- Where I have quoted from the work of others, the source is always given. With the exception of such quotations, this thesis is entirely my own work.
- I have acknowledged all main sources of help.
- Where the thesis is based on work done by myself jointly with others, I have made clear exactly what was done by others and what I have contributed myself.

Signed: _____

A.v.v. Kalunur

Date: _____

04/12/2019

MINNESOTA STATE UNIVERSITY, MANKATO

2019

Abstract

Electrical and Computer Engineering Technology

Master of Science

The concept of Substrate Integrated Circularly Polarized Waveguide

by Venkata Naga Kalyan Ram Akunuru

In this thesis, a new type of Substrate Integrated Waveguide for Horn Antennas is proposed for implementing circularly polarization on printed circuit boards. E-plane type of circuits cannot be realized by the conventional substrate integrated waveguide. Substrate integrated E-plane waveguide consists of two circuit boards attached to each other by the two copper strips which are inserted in between two circuit boards, where plated through holes are penetrated through them along the transmission direction. The plated through holes and copper strips altogether played as side walls of a conventional waveguide to support longitudinal and vertical currents. Circular Polarization has its advantages over linear polarization and it is widely implemented in many industries. Circular Polarization needs to have two fields orthogonal to each other and this novel structure is designed in a way such that it uses the concept of Substrate Integrated E-plane waveguide concept and actuates the two fields with single excitation and they will achieve orthogonality along the direction of propagation. First design achieves LHCP (Left Hand

Circularly Polarized Wave) and in the second design, a polarizer has been modeled which introduces further phase delay between the two fields such that RHCP (Right Hand Circularly Polarized Wave) is achieved. This research has been leveraged by using HFSS ANSYS modelling and simulation software.

Acknowledgements

First of all, I would like to thank my academic advisor, Dr. Xuanhui Wu who have always helped me in understanding the concepts of Microwave Engineering and also trained me in using HFSS ANSYS. His office door was always open for whenever I had questions in finishing this thesis. He consistently allowed this paper to be my own work, and steered me in the right direction whenever he thought I needed it. He has been more than an advisor, a mentor, a friendly persona and I can say that I would never have accomplished this without his patient guidance.

I would also like to thank my committee members Dr. Qun Zhang and Dr. Puteri Megat Hamari, for their advice and support. They also gave me advices along the way in my Master's study.

Finally, I must express my profound gratitude to my parents (Hare Krishna and Padmavathi) and my brother (Koundinya) for providing me with unfailing support emotionally and financially and constant encouragement throughout the years. They are the sole reason I could finish my Master's study. Thank you.

Table of Contents

1	Introduction.....	1
1.1	Transmission Lines	1
1.2	Conventional Waveguide Circuit.....	1
1.3	Substrate Integrated Waveguide (SIW) Technique.....	3
1.3.1	SIW Design Rule	5
1.3.2	Drawbacks in using SIW Design	5
2	Substrate Integrated E-plane waveguide.....	9
2.1	Circular Polarization	9
3	Substrate Integrated Circularly Polarized Waveguide.....	14
3.1	SMA Adaptor to excite circularly Polarized wave in SIEW.....	14
3.1.1	Simulated Results of the Adaptor Section	17
3.2	Polarizer section	19
3.2.1	Simulated Results.....	21
3.3	Horn Section.....	22
3.3.1	Simulated Results.....	23
3.4	Substrate Integrated LHCP Waveguide	25
3.4.1	Geometry of the Substrate Integrated LHCP waveguide.....	25

3.4.2	Simulated Results.....	26
3.5	Substrate Integrated RHCP Waveguide	29
3.5.1	Geometry of Substrate Integrated RHCP Waveguide	29
3.5.2	Simulated Results.....	30
4	Conclusion.....	33
5	References	34

List of Figures

FIGURE 1.1 RECTANGULAR WAVEGUIDE.....	2
FIGURE 1.2 MICROSTRIP LINE MODEL.....	2
FIGURE 1.3 COAXIAL LINE MODEL.....	3
FIGURE 1.4 BASIC STRUCTURE OF SIW.....	4
FIGURE 1.5 E-PLANE, H-PLANE AND TRANSVERSE PLANE IN RECTANGULAR WAVEGUIDE.....	4
FIGURE 1.6 A)H-PLANE WAVE GUIDE CIRCUIT IMPLEMENTATION OF H-PLANE WAVEGUIDE CIRCUIT	B) SIW 6
FIGURE 1.7 A)PLANAR E-PLANE WAVEGUIDE CIRCUIT B)SIW IMPLEMENTATION OF E-PLANE WAVEGUIDE CIRCUIT	6
FIGURE 1.8 (A) 3-D GEOMETRY AND (B) TOTAL ELECTRIC FIELD DISTRIBUTION IN THE MIDDLE LAYER OF AN E-PLANE SIW HORN ANTENNA	7
FIGURE 2.1 SIEW IMPLEMENTATION.....	11
FIGURE 2.2 ELECTRIC FIELD DISTRIBUTION IN TE ₁₀ MODE IN SIW CIRCUIT	11
FIGURE 2.3 E-FIELD STRENGTH AT (X,Y,Z)=(0,0,0) SHOWING CIRCULAR POLARIZATION	12
FIGURE 2.4 LHCP AND RHCP FIELD ROTATION VISUALIZATION	13

FIGURE 3.1 CROSS-SECTION VIEW OF SIEW TO SMA TRANSITION ADAPTER	14
FIGURE 3.2 3D MODEL OF THE SMA TO SIEW ADAPTOR	15
FIGURE 3.3 TOP VIEW OF SMA TO SIEW ADAPTOR SHOWING CENTER POST AND T-SHAPED COPPER STRIP	16
FIGURE 3.4 S11 OF THE ADAPTOR	17
FIGURE 3.5 S21 OF THE ADAPTOR	18
FIGURE 3.6 PHASE OF S21	18
FIGURE 3.7 CROSS SECTIONAL VIEW OF POLARIZER SECTION.....	19
FIGURE 3.8 3D MODEL OF POLARIZER SECTION	20
FIGURE 3.9 S11 OF THE POLARIZER.....	21
FIGURE 3.10 PHASE DIFFERENCE PLOT FOR POLARIZER SECTION.....	21
FIGURE 3.11 CROSS SECTIONAL VIEW OF HORN SECTION	22
FIGURE 3.12 3D MODEL OF HORN SECTION.....	23
FIGURE 3.13 S11 OF THE HORN SECTION.....	24
FIGURE 3.14 GAIN PLOT FOR THE HORN SECTION	24
FIGURE 3.15 CROSS SECTIONAL VIEW OF LHCP TYPE WAVEGUIDE.....	25
FIGURE 3.16 3D GEOMETRY OF SUBSTRATE INTEGRATED LHCP WAVEGUIDE	26
FIGURE 3.17 $ S_{11} $ OF SUBSTRATE INTEGRATE LHCP WAVEGUIDE	27

FIGURE 3.18 AXIAL RATIO PLOT FOR SUBSTRATE INTEGRATED LHCP WAVEGUIDE	27
FIGURE 3.19 LHCP VS RHCP GAIN PLOT FOR SUBSTRATE INTEGRATED LHCP WAVEGUIDE	28
FIGURE 3.20 CROSS SECTIONAL VIEW OF RHCP TYPE WAVEGUIDE.....	29
FIGURE 3.21 3D GEOMETRY OF SUBSTRATE INTEGRATED RHCP WAVEGUIDE.....	30
FIGURE 3.22 $ S_{11} $ OF SUBSTRATE INTEGRATED RHCP WAVEGUIDE.....	31
FIGURE 3.23 AXIAL RATIO PLOT FOR SUBSTRATE INTEGRATED RHCP WAVEGUIDE	32
FIGURE 3.24 RHCP VS LHCP GAIN PLOT FOR SUBSTRATE INTEGRATED RHCP WAVEGUIDE	32

List of Abbreviations

TE	Transverse Electric
TM	Transverse Magnetic
TEM	Transverse Electro-Magnetic
SIW	Substrate Integrated Waveguide
SIEW	Substrate Integrated E plane Waveguide
LHCP	Left Hand Circularly Polarized
RHCP	Right Hand Circularly Polarized

1 Introduction

1.1 Transmission Lines

In electromagnetics and Electrical Engineering, a transmission line is usually considered as pair of electrical conductors designed to carry signal in high frequencies or Microwave frequencies. Transmission lines that consist of two or more conductors may support transverse electromagnetic (TEM) waves, characterized by the lack of longitudinal field components [1]. Waveguides, often consisting of a single conductor, support transverse electric (TE) and/or transverse magnetic (TM) waves, characterized by the presence of longitudinal magnetic or electric field components.

There are several commonly used transmission lines shown in which includes coaxial lines (Figure 1.3), micro strip lines (Figure 1.2) and waveguides (Figure 1.1).

1.2 Conventional Waveguide Circuit

Since, transmission lines are used at high frequencies, its behavior will be quite different at low frequency transmissions considering the wave nature into account.

Among all the mentioned transmission lines, waveguide as shown in Figure 1.1 has outstanding performance. Waveguide, in usual consists of a hollow pipe made of metal which is filled with air or any other dielectric substrate in the cavity. Unlike Transmission lines which can support TEM waves, waveguides can only support TE or TM modes of propagation. The reason is explained in [2]. Therefore, if both electric and magnetic components are transverse to wave propagation direction, wave cannot propagate.

Generally speaking, the conventional waveguide has got two typical structures called as E-plane waveguide and H- plane waveguide. In the Figure 1.5 we can see a rectangular waveguide cross section which defines 3 planes in a rectangular waveguide. In E – plane circuit, the electric field is horizontally polarized and in H – plane circuit the magnetic field is horizontally polarized and parallel to the ground plane. In both the circuits, it is assumed that only the fundamental mode is excited so that electromagnetic waves are reflected because electromagnetic waves cannot pass through conductors but reflected by the conductors.

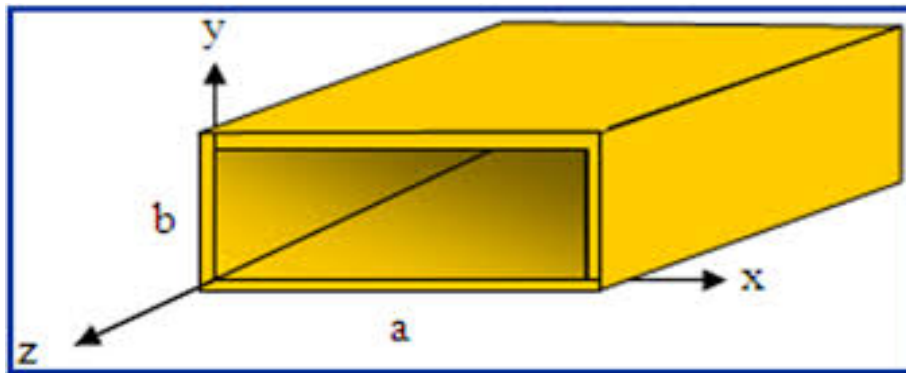


Figure 1.1 Rectangular Waveguide

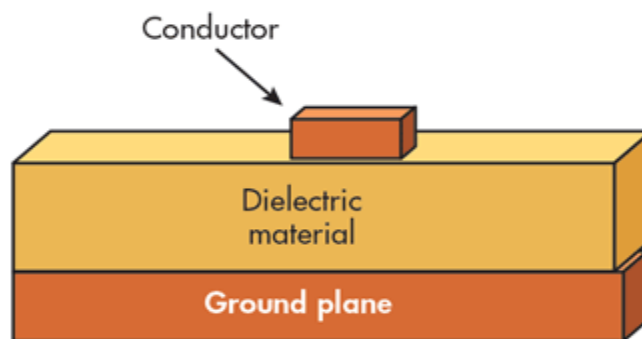


Figure 1.2 Microstrip line model

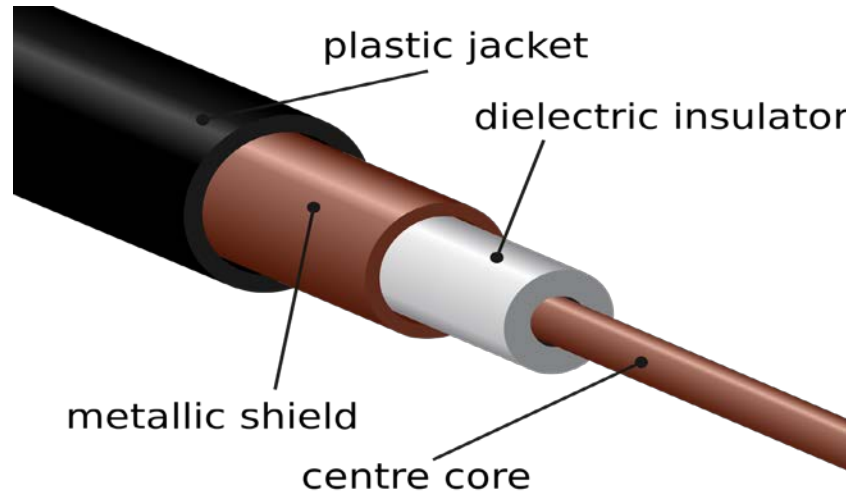


Figure 1.3 Coaxial Line Model

Source: https://en.wikipedia.org/wiki/Coaxial_cable

1.3 Substrate Integrated Waveguide (SIW) Technique

SIW is a technique that has been of interest and studied extensively [3]- [4]. It is used for implementing of planar waveguide circuits on a Printed Circuit Board. This concept was first demonstrated in [5]. The two metal plates on the PCB are emulated as the top and bottom walls of the waveguide to support horizontal and longitudinal current based on the boundary condition $\hat{n} \times \vec{H} = \vec{J}_s$. As shown in the Figure 1.4, metal holes are drilled along the PCB. These metal holes are used to emulate the vertical walls of a waveguide. These conclusions are taken from [6].

Since its invention, many devices such as filters [7]- [8], diplexers [9], power dividers [10]- [11] and so on. Slot antennas can also be modeled [12]- [13] and even has many wide band applications. One of the disadvantage using this method is that it cannot support E-plane type waveguide circuit because, electric field is parallel to the planar circuit and it will cause leakage in signal between the through holes drilled on the PCB. E-plane and H-plane in a Rectangular waveguide can be visualized from the Figure 1.5.

To overcome this, substrate integrated E-plane waveguide (SIEW) was invented recently [14] which is discussed briefly later.

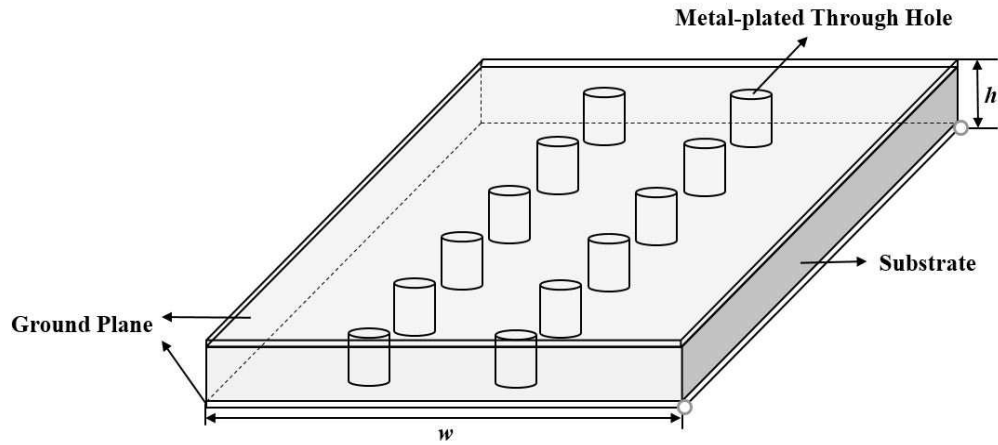


Figure 1.4 Basic structure of SIW

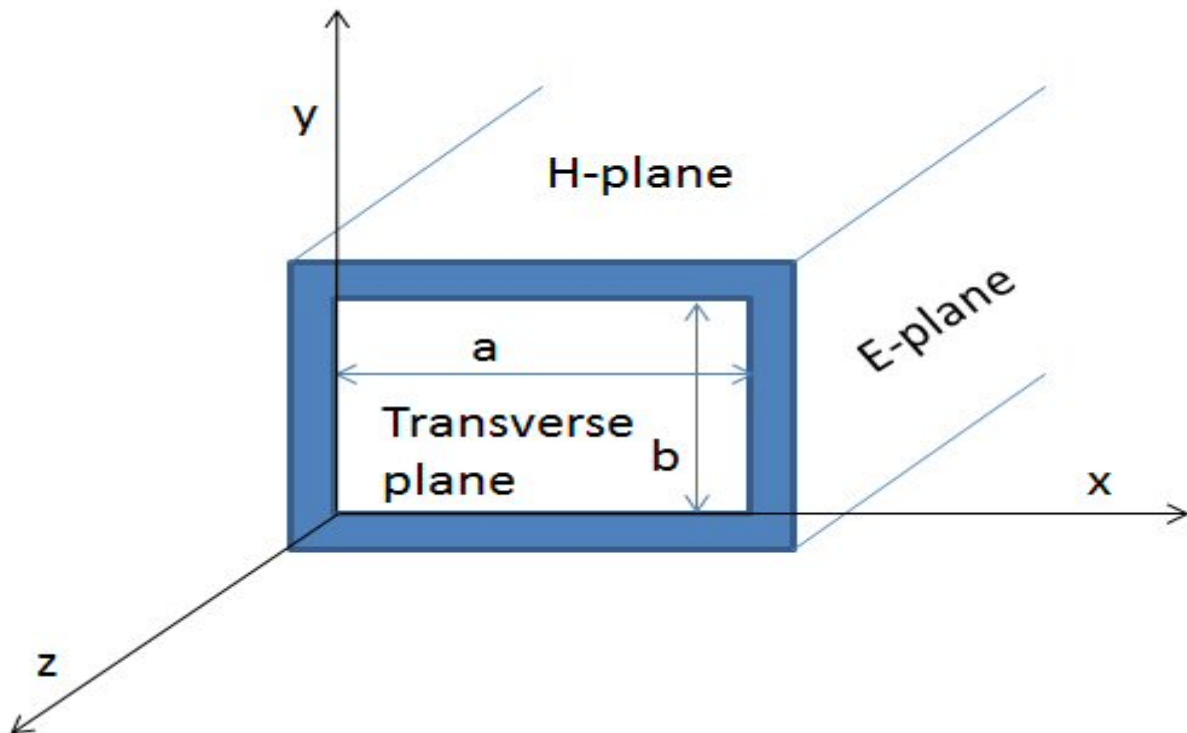


Figure 1.5 E-plane, H-plane and Transverse Plane in Rectangular waveguide

1.3.1 SIW Design Rule

Two rows of metallized holes are placed along the substrate during synthesizing of Rectangular waveguide as explained in [5]. The diameter D of the holes, the spacing b between the holes and the spacing W between the two rows are the physical parameters necessary for the design of the guide. The pitch b must be kept small to reduce the leakage loss between adjacent posts. However, the post diameter D is also subject to the loss problem. As a result, the ratio D/b is considered to be more critical than the pitch length because the post diameter and the pitch length are interrelated as mentioned in [3].

1.3.2 Drawbacks in using SIW Design

As already mentioned, one of the major disadvantages using this method is it cannot realize E-plane type of waveguide where the Electric field is parallel to the planar circuit. E-plane waveguides are used widely in microwave industry [15]- [16]. One of the major reasons of implementing E-plane waveguide is because it has length of less than half a wavelength thereby leaving lesser footprint on 2-D plane. Therefore many applications are developed like diplexers [17], Resonators [18], power dividers that work in W-band [19] and there has also been recent development for hybrid metal insert filters for millimeter-wave applications [20] and so on. Because of all these advantages, implementing an E-plane waveguide on a PCB is extremely useful.

The reason that it cannot realize E-field is determined already in papers [6] [7] [21] [22]. To put in rather simpler terms, E-plane type waveguide gives narrow beam in E-field and broad beam in H-field. If we try to implement E-plane type waveguide in SIW, all the energy escapes between the via gaps as shown in Figure 1.8 .

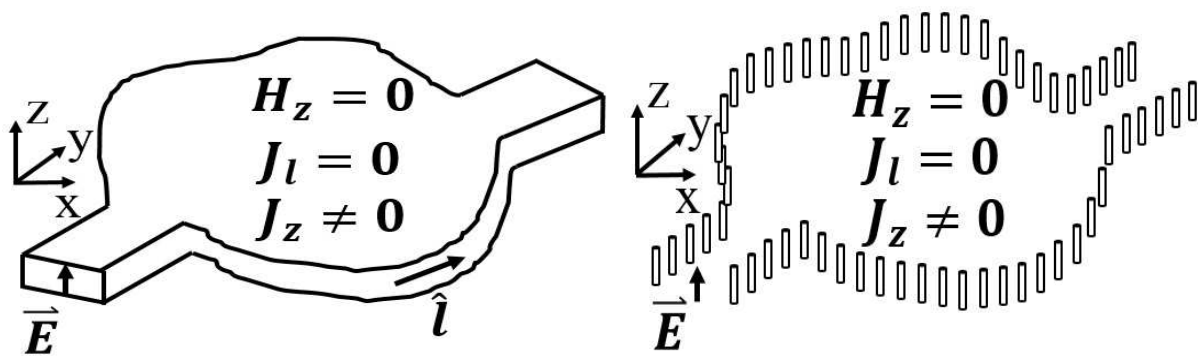


Figure 1.6 a)H-plane wave guide circuit

b) SIW implementation of H-plane waveguide circuit

Reprinted from Michael Hedin ; Danyang Huang ; Xuan Hui Wu ; Qun Zhang, "Substrate Integrated E-Plane Waveguide (SIEW) to Design E-Plane and Dual Polarized Devices", IEEE Transactions on Antennas and Propagation, published in Dec, 2018

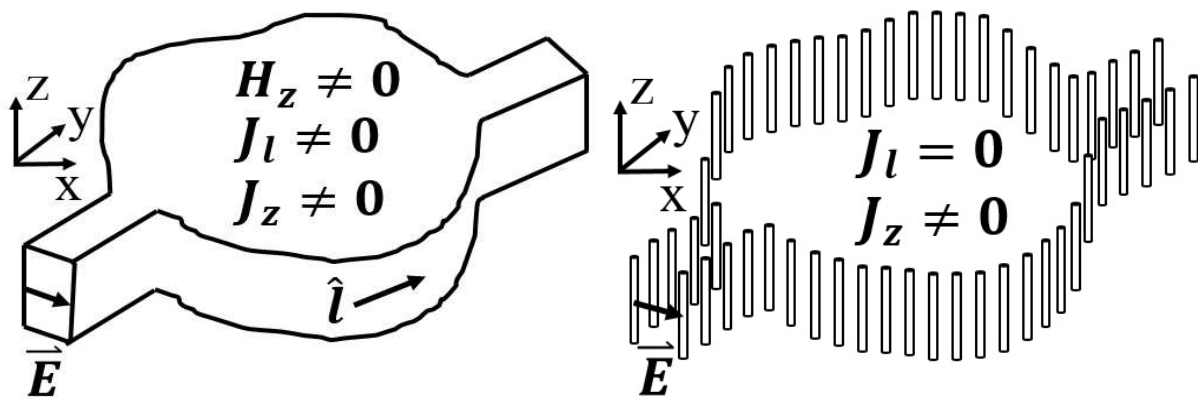


Figure 1.7 a)Planar E-plane waveguide circuit b)SIW implementation of E-plane waveguide circuit

Reprinted from Michael Hedin ; Danyang Huang ; Xuan Hui Wu ; Qun Zhang, "Substrate Integrated E-Plane Waveguide (SIEW) to Design E-Plane and Dual Polarized Devices", IEEE Transactions on Antennas and Propagation, published in Dec, 2018

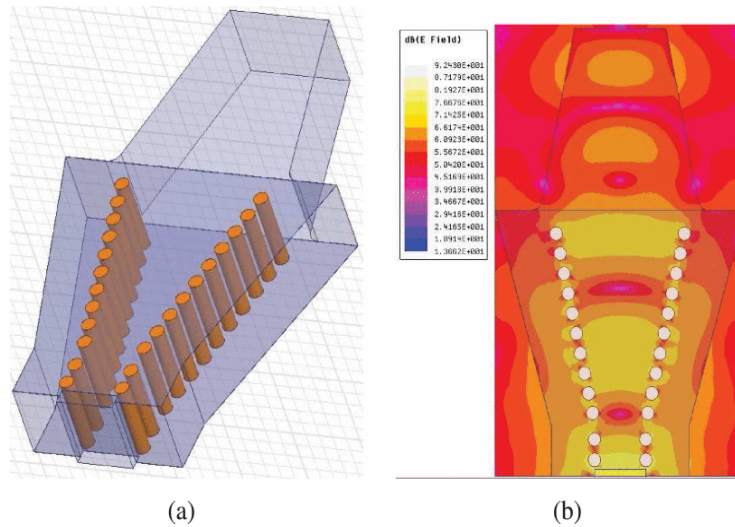


Figure 1.8 (a) 3-D geometry and (b) total electric field distribution in the middle layer of an E-plane SIW horn antenna

Reprinted from Zhewei Gu ,X.H.Wu, Qun Zhang “Substrate Integrated E-plane Waveguide Horn Antenna and Antenna Array” , IEEE Transactions on Antennas and Propagation, published in March,2018

An H-plane waveguide circuit is placed on the xy plane, as shown in Figure 1.6. It is excited by an H-plane waveguide port under TE₁₀ mode so that the excited electric field is in the z -direction only and is independent of the z coordinate. Because of the constant height of the structure, $E_x = E_y = 0$ in the entire circuit, which leads to $H_z = 0$ based on the Maxwell equation

$$\nabla \times \bar{E} = -j\omega\mu\bar{H} \quad (1)$$

On any vertical wall, the longitudinal current density is given by $J_l = H_z = 0$ due to boundary condition $\vec{J} = \hat{n} \times \vec{H}$ assuming the longitudinal current is tangential to the vertical wall and is also orthogonal to z - direction. Hence the through holes drilled across the substrate are enough for flowing of current in z -direction. If we implement the same type of design for E-plane type waveguide, the results are unsatisfactory.

Figure 1.7 shows an E-plane waveguide, where the wide walls are vertical and narrow walls are horizontal. This type of current cannot be supported when taken SIW because the wave cannot see the vertical through holes drilled as a vertical wall. It sees them as slot antennas and hence escapes becoming very lossy as shown in Figure 1.8.

The Electric field existing in circuit can be expressed as

$$\vec{E}(x, y, z) = [\hat{x}E_x(x, y) + \hat{y}E_y(x, y)]\sin(k_z z) \quad (2)$$

where $k_z = \frac{\pi}{4}$ is the thickness of the circuit . Substituting eq. 2 in eq. 1 gives the magnetic field as

$$\begin{aligned} \vec{E}(x, y, z) = & \frac{j}{\omega\mu} \{ \hat{x}k_z E_y(x, y) \cos(k_z z) + \hat{y}k_z E_x(x, y) \cos(k_z z) \\ & + \hat{z} \sin(k_z z) [\frac{\partial}{\partial x} E_y(x, y) - \frac{\partial}{\partial y} E_x(x, y)] \} \end{aligned} \quad (3)$$

As we know that the electric current density on the vertical walls equals the tangential magnetic field, but rotates 90°, there exists both vertical current density J_z and longitudinal current density J_l as

$$J_z = \frac{jk_z \cos(k_z z)}{\omega\mu} [\hat{x}E_y(x, y) - \hat{y}E_x(x, y)]. \hat{l} \quad (4)$$

$$J_l = \frac{j \sin(k_z z)}{\omega\mu} [\frac{\partial}{\partial x} E_y(x, y) - \frac{\partial}{\partial y} E_x(x, y)] \quad (5)$$

where \hat{l} is unit vector in the longitudinal direction of the vertical wall. The vertical current J_z in the eq. 4 is supported by the copper plated through holes in Figure 1.6 , but there is no structure that supports that allows longitudinal current J_l in eq. 5 .

2 Substrate Integrated E-plane waveguide

As SIW structure can just actualize H-plane sort waveguides and neglect to execute E-plane sort waveguides, idea of SIEW technique has been tended to [22]. In this, another structure is acquainted into existing plan with help longitudinal current. This is a multilayer PCB innovation wherein copper strips are embedded in the middle of the waveguide circuit which goes about as extra way for electric flow. Ideal tallness on which the strips are put is resolved dependent on the electrical flow thickness on the vertical dividers. As longitudinal current has sinusoidal dispersion in z-direction, the peak value is supposed to be at the center and subsequently the copper strips are put in the center layer in the multilayer PCB stacking. This encourages the longitudinal current to stream along the vertical walls to help the flow of the current. This kind of configuration is alluded to as Substrate Integrated E-plane waveguide as appeared in Figure 2.1. As appeared in Figure 2.2, the Electric field circulation is supported by the Copper strips in the middle.

2.1 Circular Polarization

The Polarization of an antenna is the polarization of radiated fields produced by an antenna, evaluated in far field. Hence, antennas are often classified as “Linearly Polarized” or a “Right Hand Circularly Polarized Antenna”. Supposing that the E-field of a plane wave is given by the equation

$$\mathbf{E} = \cos(2\pi f \left(t - \frac{z}{c}\right))\hat{x} + \sin(2\pi f \left(t - \frac{z}{c}\right))\hat{y} \quad (6)$$

If we consider the above equation, the x- and y- components are 90 degrees out of phase. If the field is observed at $(x,y,z)=(0,0,0)$, the plot of E-field would look like Figure 2.3. We can notice that E-field is rotating in circle. This type of field is described as Circularly Polarized Wave.

There are three main criteria required to be met for having circular polarization. They are

- The E-field must have two orthogonal (perpendicular) components.
- The E-field's orthogonal components must be of equal magnitude.
- The orthogonal components must be 90 degrees out of phase.

If the wave in Figure 2.3 is travelling out of this paper, the field is rotating in the counter-clockwise direction and is termed as **Right Hand Circularly Polarized (RHCP)**. If the fields were rotating in the clockwise direction, the field would be **Left Hand Circularly Polarized (LHCP)**.

The straightforward idea discussed above is imperative for antenna to antenna correspondence. Initial, a horizontally polarized antenna won't communicate with a vertically polarized antenna. Because of the reciprocity theorem, antennas transmit and receive in the very same way. Henceforth, a vertically polarized antenna transmits and receives vertically polarized fields. Therefore, if a horizontally polarized antenna is attempting to communicate with a vertically polarized antenna, there will be no reception.

In general, for two linearly polarized antennas that are rotated from each other by an angle Φ , there will be a power loss due to this polarization mismatch and it is described by **Polarization Loss Factor (PLF)** and is given as

$$PLF = \cos^2 \Phi \quad (7)$$

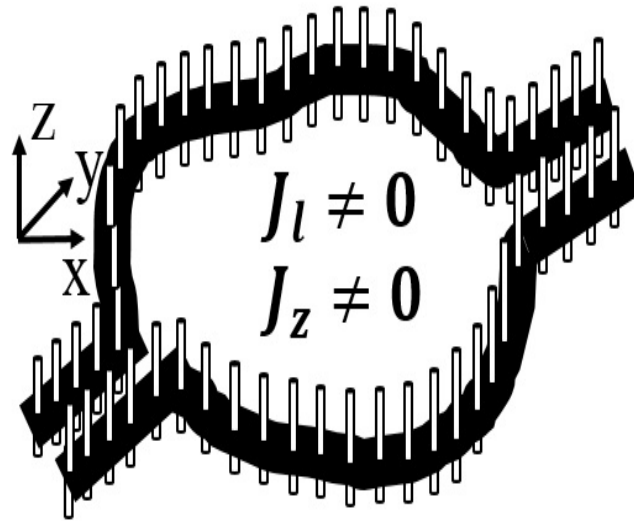


Figure 2.1 SIEW implementation

Reprinted from Michael Hedin ; Danyang Huang ; Xuan Hui Wu ; Qun Zhang, “Substrate Integrated E-Plane Waveguide (SIEW) to Design E-Plane and Dual Polarized Devices”, IEEE Transactions on Antennas and Propagation, published in Dec, 2018

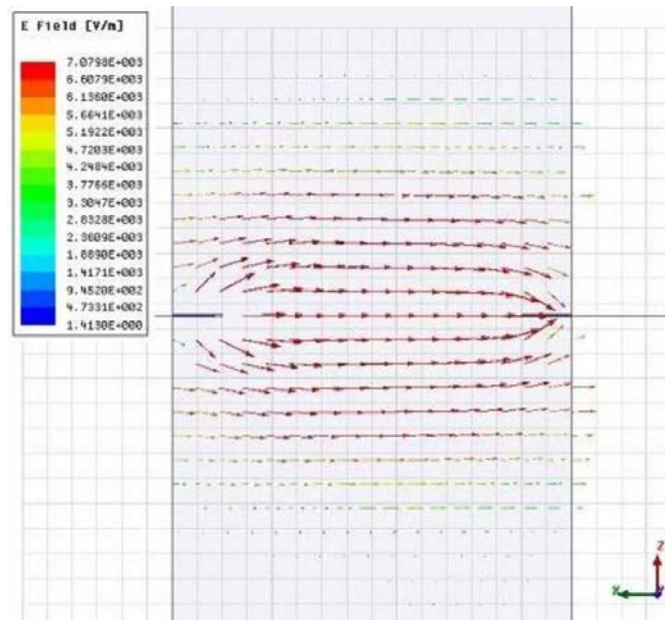


Figure 2.2 Electric field distribution in TE₁₀ mode in SIW circuit

Reprinted from “Concept of Substrate Integrated E-plane Waveguide and Waveguide filter” by D.Huang, X.H. Wu and Q.Zhang, International Workshop on Antenna Technology: Small Antennas, Innovative Structures and Applications, Cocoa Beach, FL, USA , Feb. 29- Mar. 2 , 2016.

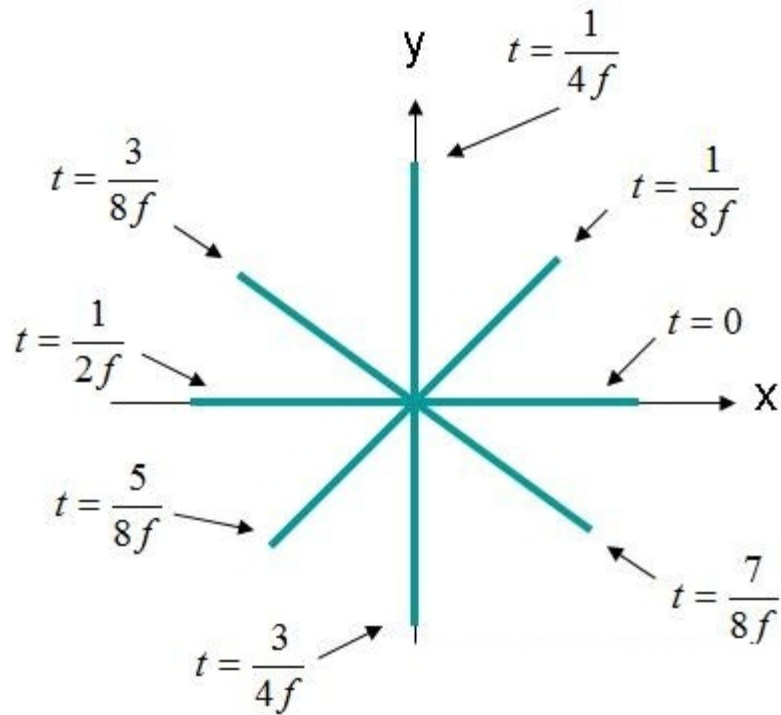


Figure 2.3 E-field strength at $(x,y,z)=(0,0,0)$ showing Circular Polarization

From Eq. 7, we can deduce that if the antennas have same polarization and there is no deviation in the angle between transmitting and receiving antenna, there is no power loss due to polarization mismatch. If one antenna is vertically polarized and other is horizontally polarized, the angle is 90 degrees and no power will be transferred.

Circular polarization is a desirable characteristic for many antennas. Two antennas that are both circularly polarized don't endure signal loss because of polarization mismatch. Another preferred standpoint of circular polarization is that a RHCP wave will reflect off a surface and be LHCP [23]. This is favorable on the grounds that an antenna intended to receive RHCP waves will have some invulnerability to the signal-fading impacts of reflected waves meddling with the desired wave. These are some of the reasons GPS signals from satellites are RHCP. There are many applications that have been discussed such as Filters [24] , Polarizer [25], slot antennas [26].

CP Electric Field Rotation Sense

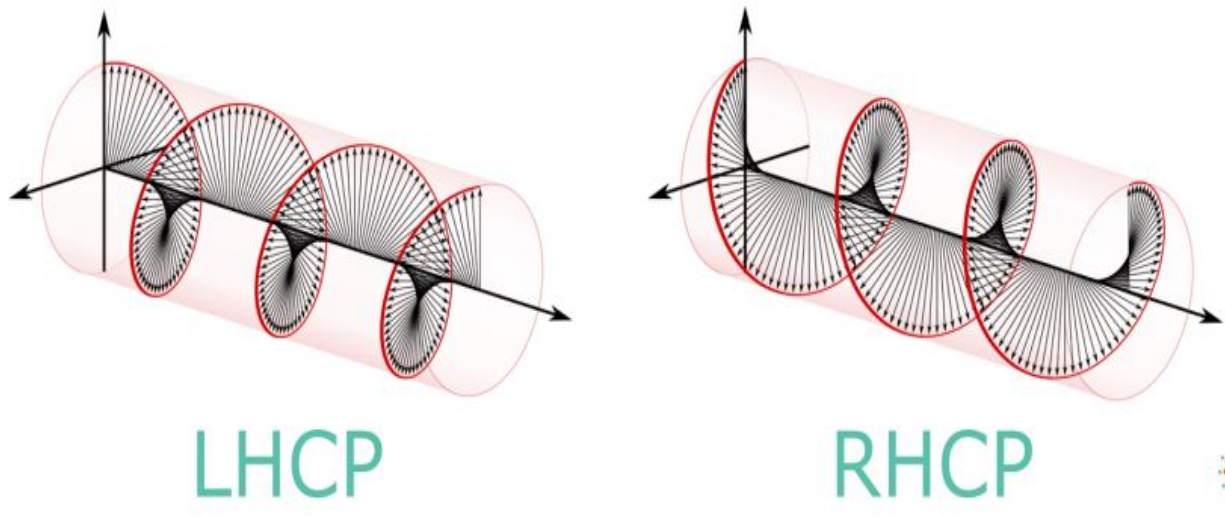


Figure 2.4 LHCP and RHCP field rotation visualization

Source: <https://antennatestlab.com/wp-content/uploads/2017/09/CP-Explained-Without-Math.pdf>

As discussed before, circularly polarized wave has numerous applications, it is imperative that this innovation should be investigated more and from now on this report is tied in with designing and prototyping of a Substrate Integrated circularly polarized waveguide. It has the upsides of utilizing of Substrate Integrated Waveguide joined with the advantages of having circular polarized wave. Rest of the paper has been isolated into following segments

- Adapter for transitioning of SIEW to Circularly Polarized Wave
- Geometry
- Designing of Polarizer for attaining RHCP wave
- Simulated Results
- Designing of Horn section and simulated Results
- Final results and Conclusion

3 Substrate Integrated Circularly Polarized Waveguide

3.1 SMA Adaptor to excite circularly Polarized wave in SIEW

All of the models in this thesis are designed and all the performance evaluations are done using help of HFSS ANSYS modelling software. The waveguide is built by binding of Rogers TMM3 substrate which is an anisotropic material and of same thickness of $h= 3.175\text{mm}$. Top board has copper plating on the top side and the bottom board has copper plating on the top as well as the bottom sections.

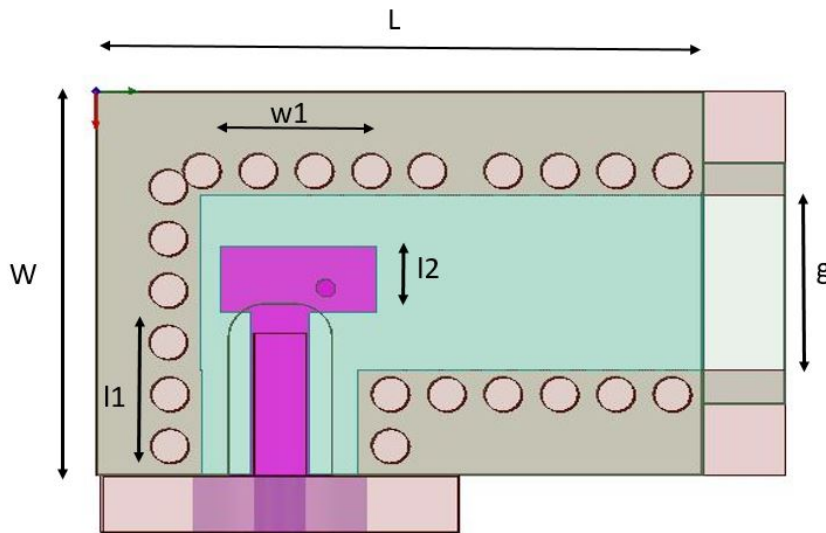


Figure 3.1 Cross-section view of SIEW to SMA transition adapter

$$W= 11.09081599\text{mm}, L= 16.11965951\text{mm}, l_1= 4.702675177\text{mm}, l_2=1.922153885\text{mm}, \\ w_1=4.16618206\text{mm}, g= 5.046711936\text{mm}$$

As confirmed by the PCB manufacturer, the dielectric constant $\epsilon_{rx} = \epsilon_{ry} = 3.4$, $\epsilon_{rz}=3.45$ and loss tangent $\tan \delta_x = \tan \delta_y = \tan \delta_z = 0.002$ are used. The top and bottom surfaces are copper plated because they emulate top and bottom walls of a conventional waveguide. Series of copper-plated

through holes are drilled along the wave propagation direction as shown in Figure 3.1 . All through holes have same radius $r=0.5\text{mm}$ and the spacing between the holes are carefully optimized [4] . Since, the failure of SIW to actualize E-plane circuits because of the absence of physical structure to bolster longitudinal current, copper strips are implanted in between the circuit boards, where the peak value of the sinusoidal current distribution of the TE₁₀ mode. A feeding network which includes an SMA adapter and a short SIEW section is employed which is referred to as SIEW to SMA transition. The dimensions of this transition is modelled using HFSS ANSYS software as shown in Figure 3.1.

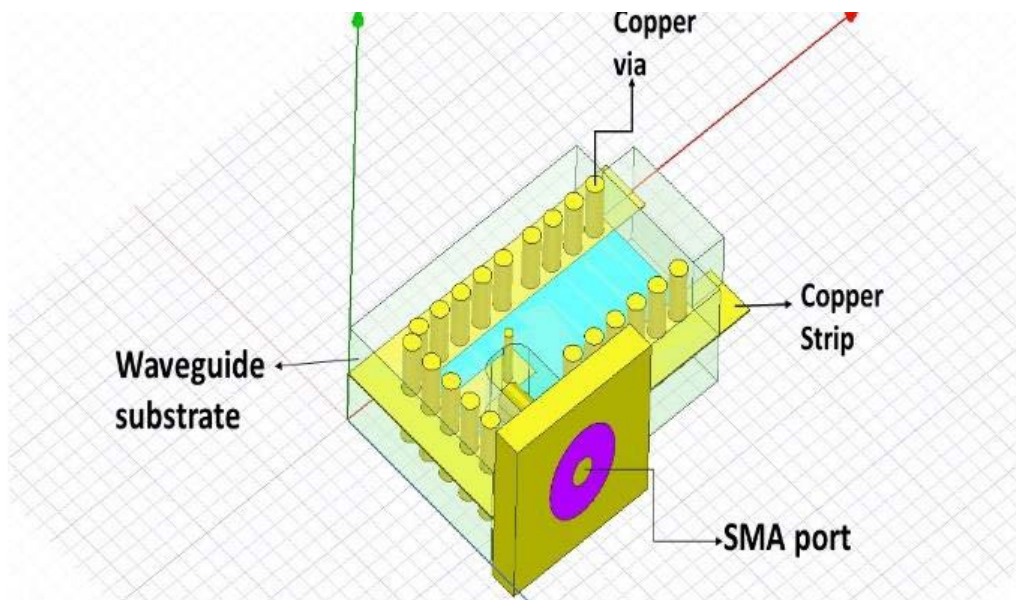


Figure 3.2 3D model of the SMA to SIEW adaptor

The benefits of having circular polarization has been discussed in the earlier chapters. We need two components to achieve circular polarization which are orthogonal and of equal magnitude. In this novel structure, there is just a single excitation and Figure 3.2 shows the cross sectional view at the interface of the two boards. A 'T' shape copper strip is inserted in the middle layer for the soldering of the SMA adaptor's inner conductor. Its shape and location is optimized to achieve good impedance matching. It also excites the horizontal component of the electric field

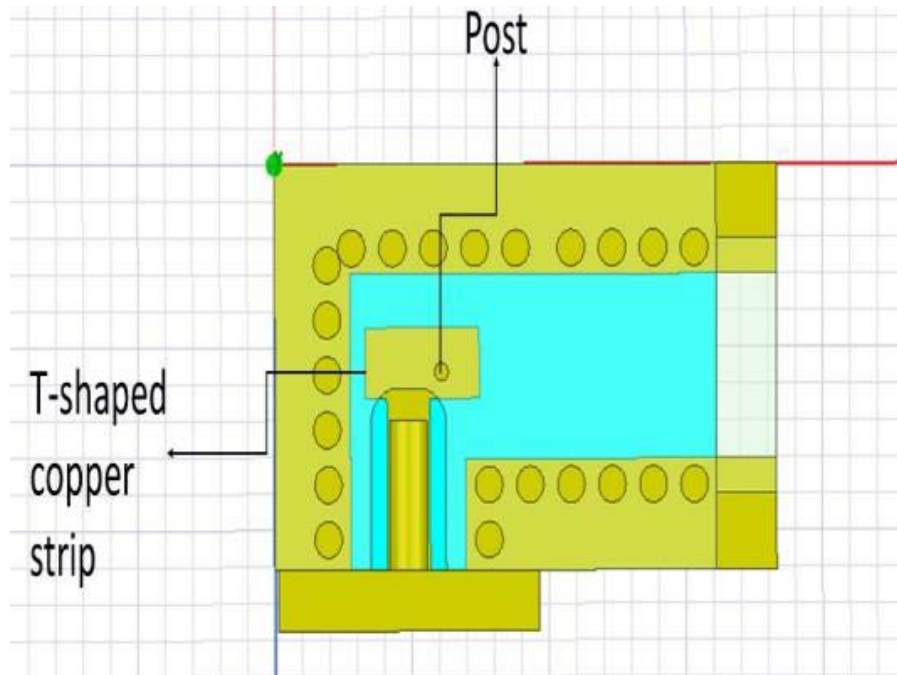


Figure 3.3 Top view of SMA to SIEW adaptor showing center post and T-shaped copper strip

As shown in the Figure 3.3, a copper plated through hole is drilled in the top PCB and is electrically connected to both the ‘T’ shaped copper strip and the top copper plating layer of the PCB. The copper plated through hole excites the vertical component of the electric field. Its location is optimized together with the ‘T’ shape copper strip in order to excite equal amplitudes of electric fields for the vertical and horizontal components. The two linear orthogonal field components propagate in the SIEW with different speeds because the phase constants of the two polarizations are different. At a certain distance away from the ‘T’ shape strip, 90 degrees phase difference will be observed to achieve circularly polarized wave.

3.1.1 Simulated Results of the Adaptor Section

The adaptor is designed using ANSYS HFSS. The shape and location of the ‘T’ shape strip as well as the location of the plated through hole on the ‘T’ shape strip are vital parameters to determine the adaptor performance. Figure 3.4 and Figure 3.5 show the simulated S_{11} and S_{21} for both polarizations after optimization. As shown, the reflection coefficient is below -10dB over the 18-19GHz band. The transmission coefficient for both polarizations are at around -3.4dB over the 18.2-19GHz band. The phase of the transmission coefficients are also investigated and plotted in Figure 3.6. The phase difference of the transmission coefficients between the two polarizations is observed to be 113 degrees at 18 GHz and 78 degrees at 19 GHz, both are close to 90 degrees as required by the circularly polarized wave. The results at Figure 3.5 and Figure 3.6 demonstrates the excitation of circularly polarized wave at the output port of the adaptor.

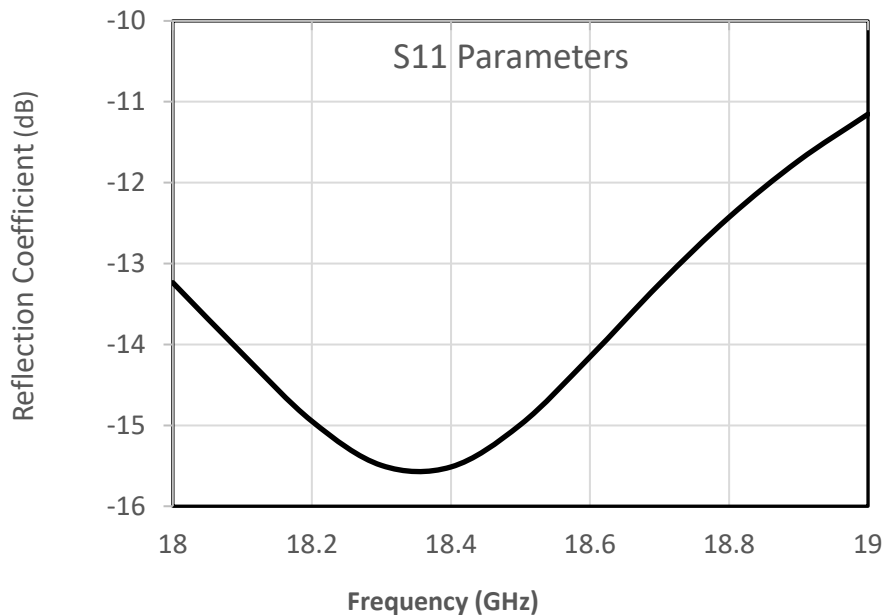


Figure 3.4 S_{11} of the adaptor

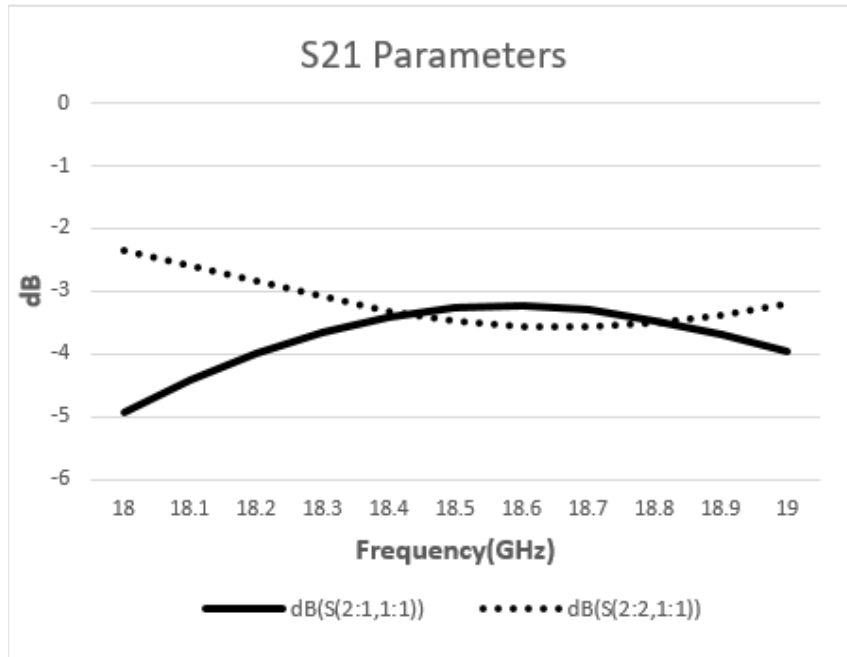


Figure 3.5 S21 of the adaptor

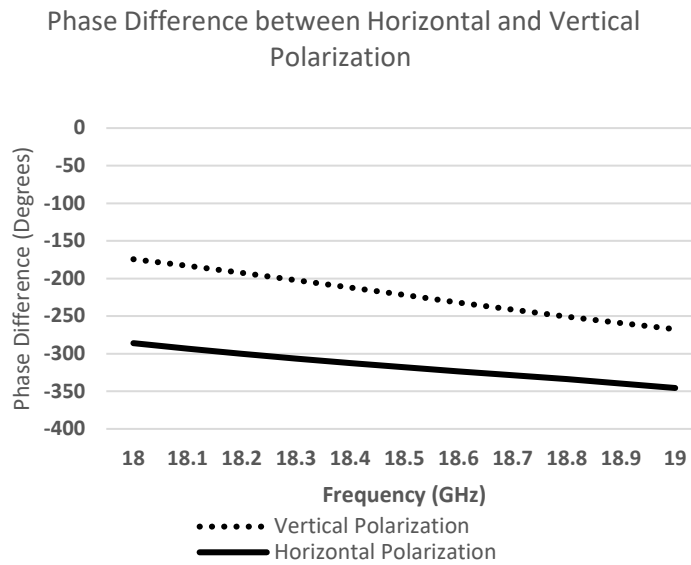


Figure 3.6 Phase of S21

In order to evaluate the transmission efficiency, the S- parameters are taken into account, which typically represents the relationship between different inputs and outputs of an electrical system. $|S_{11}|$, namely reflection coefficient represents the amount of energy reflected. Usually, a target below -10dB which means that no more than 10% of energy is reflected is considered to be a satisfactory goal during the optimization.

3.2 Polarizer section

The SMA to SIEW adaptor is used for generating the circular polarized wave as discussed earlier and also the results have been verified using HFSS ANSYS. Using the design, it would be generating LHCP(Left Hand Circularly Polarized Wave) and it will be discussed later.

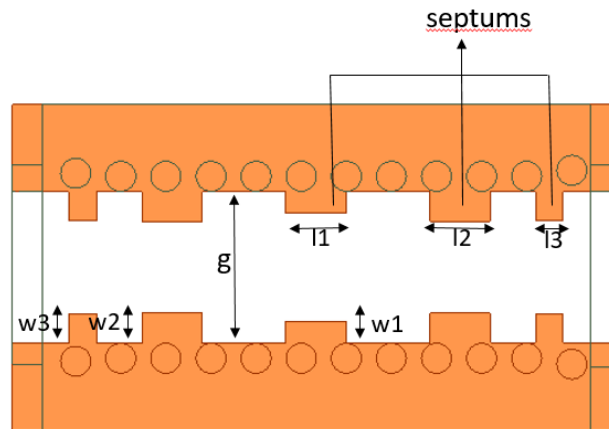


Figure 3.7 Cross sectional view of Polarizer Section

$g=5.0467\text{mm}$, $l_1=1.999697216\text{mm}$, $l_2= 2.0099\text{mm}$, $l_3 = 0.922\text{mm}$, $w_1=0.7238474262\text{mm}$, $w_2=0.994\text{mm}$, $w_3= 0.983\text{mm}$, length of the polarizer section=18.2mm, width=10.83mm
diameter of through holes=1mm

In this section, a Polarizer design has been introduced which presents a further phase delay between the two waves. Polarizer segment has septums as shown in Figure 3.7 , which are set on the copper strip in the center layer which introduces the delay we need for obtaining RHCP (Right Hand Circularly Polarized Wave). The lengths and widths of septums are optimized. During the

optimization, the goal is set such that the principal half area of the polarizer is symmetrical to the second half for the purpose of saving optimization time. The dimensions after optimization are shown in Figure 3.7.

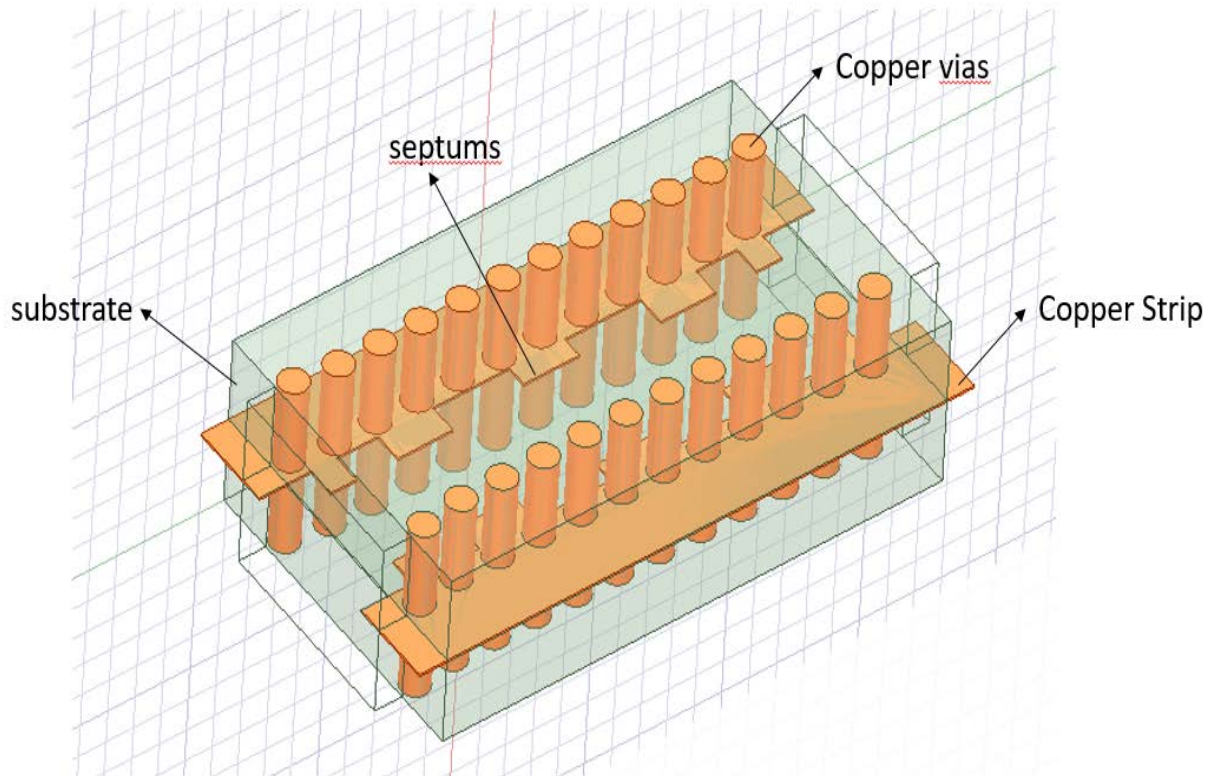


Figure 3.8 3D model of Polarizer Section

Figure 3.8 shows the 3D model of the Polarizer section. The modelling is done using HFSS ANSYS and the structure design is similar to the SIEW technology we have discussed earlier. Septums are extended from the copper strip placed on the center of the stacking of the PCB boards. The simulated results are discussed next. For obtaining the RHCP, phase difference of 270 degrees to be achieved.

3.2.1 Simulated Results

As already mentioned, positioning and the dimensions of the septums play a vital role in determining the polarizer characteristics. After number of simulations, the required result has been achieved and the dimensions are stated in Figure 3.7.

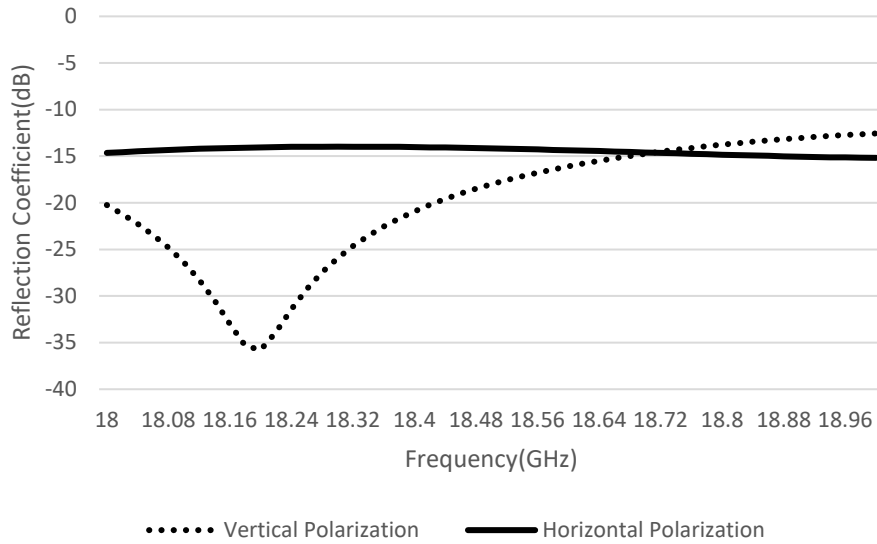


Figure 3.9 S11 of the polarizer

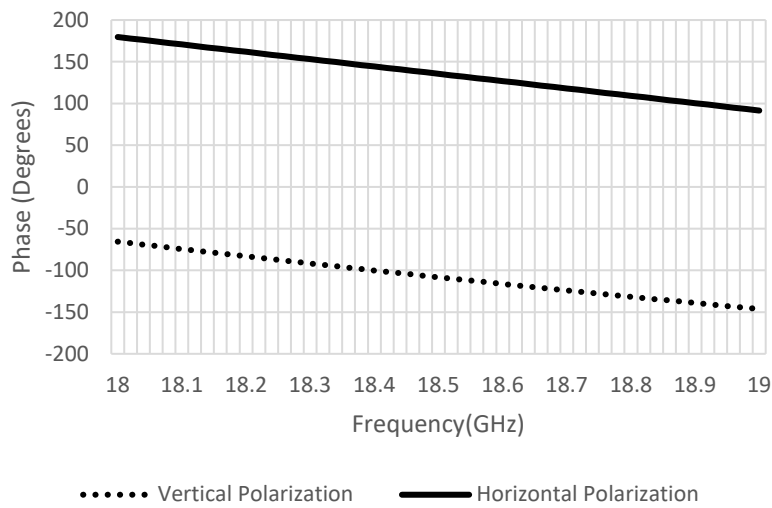


Figure 3.10 Phase Difference plot for Polarizer Section

Figure 3.9 shows that the reflection coefficient is below -20dB over the 18-19GHz band for the H-field wave and below -14dB for E-field wave. At 18.2GHz, the reflection coefficient is below -35 dB. The phase of the transmission coefficients are also investigated and plotted in Figure 3.10. The phase difference of the transmission coefficients between the two polarizations is 244 degrees at 18-18.5GHz, and 237 degrees at 19GHz, both are close to 270 degrees as required for the RHCP. This result demonstrates the excitation of circularly polarized wave from the adaptor to horn section. This section is later placed in between the adaptor and the Horn section of the waveguide and optimized for the RHCP to be achieved.

3.3 Horn Section

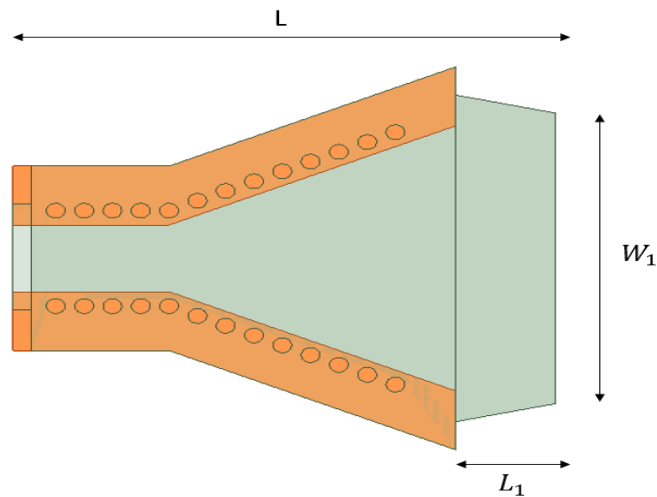


Figure 3.11 Cross Sectional view of Horn Section

$$L=27.74\text{mm}, W_1=19.6\text{mm}, L_1=5.25\text{mm}$$

Horn section is designed similar to that of all previous models implementing SIEW technology. For the sake of better impedance matching and return loss response, a trapezoidal dielectric load

is etched in front of the horn aperture for which the dimensions are mentioned in Figure 3.11. The dielectric load is supposed to minimize the reflections caused by the discontinuities between the substrate and free space at the aperture. This contributes to better reflection coefficients. Isometric view of the Horn section can be seen from Figure 3.12.

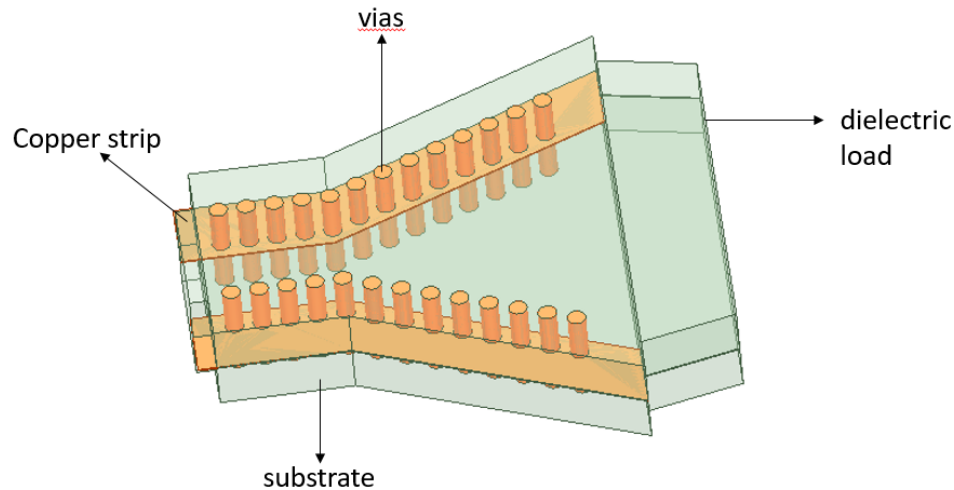


Figure 3.12 3D model of Horn Section

3.3.1 Simulated Results

The horn section has been designed by setting optimization goal for S_{11} parameters to be less than -14 dB and in the Figure 3.13, we can see that the simulation results are very good as the reflection coefficient for both the horizontal and vertical polarized waves are less than -14 dB in 18-19 GHz frequency band. Also, the gain for both the horizontal and vertical polarization waves are set to be 7dB in the wave propagation direction. We can see from Figure 3.14 that for the E-field wave, the gain is above 7.2dB in 18-19 GHz band and for the H-field wave, the gain is 7.4 dB at 18 GHz and 8.4 dB at 19 GHz.

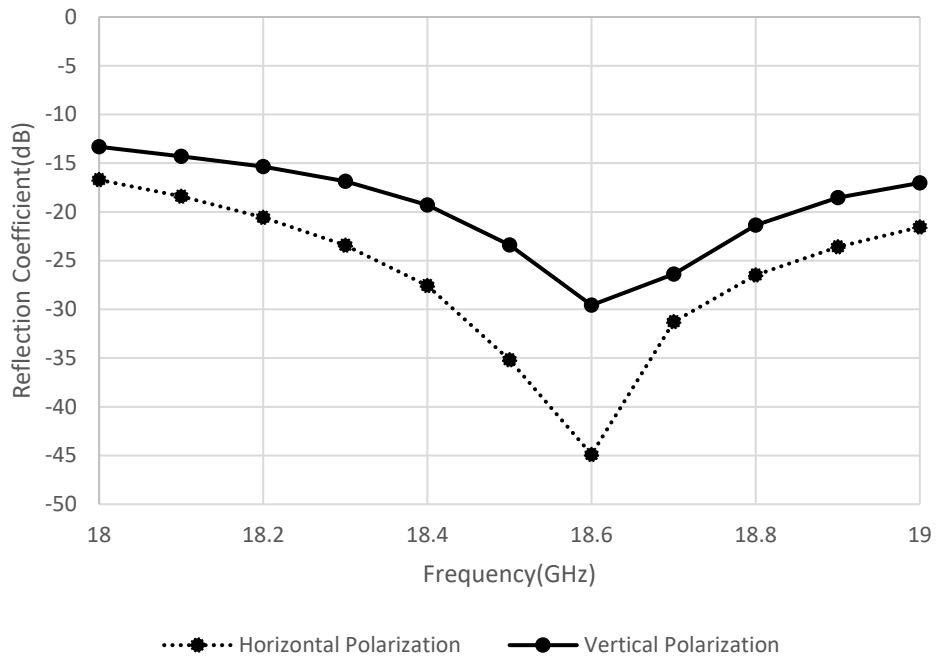


Figure 3.13 S11 of the Horn Section

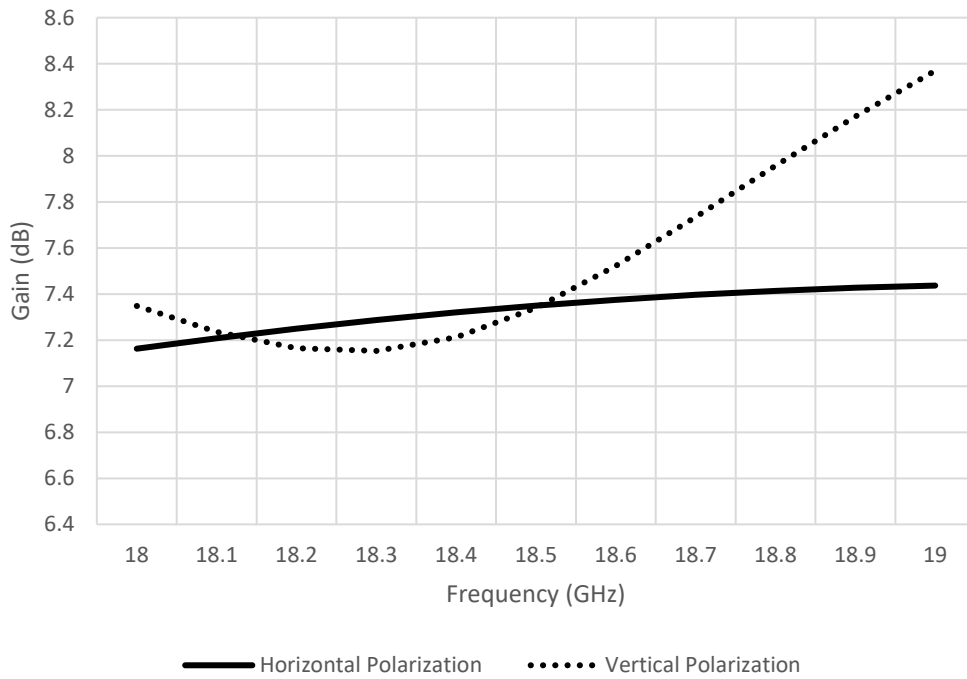


Figure 3.14 Gain Plot for the Horn Section

3.4 Substrate Integrated LHCP Waveguide

3.4.1 Geometry of the Substrate Integrated LHCP waveguide

While there are many benefits in the satellite applications for CP to CP antenna radio links, a CP to linear antenna link is also very useful. In fact, when one end of a radio link uses a CP antenna, all the rotation independent benefits of CP antennas are realized. This is advantageous considering cellular devices, because even if there is constant orientation mismatch of the cellular device, CP allows the device to get reception [23].

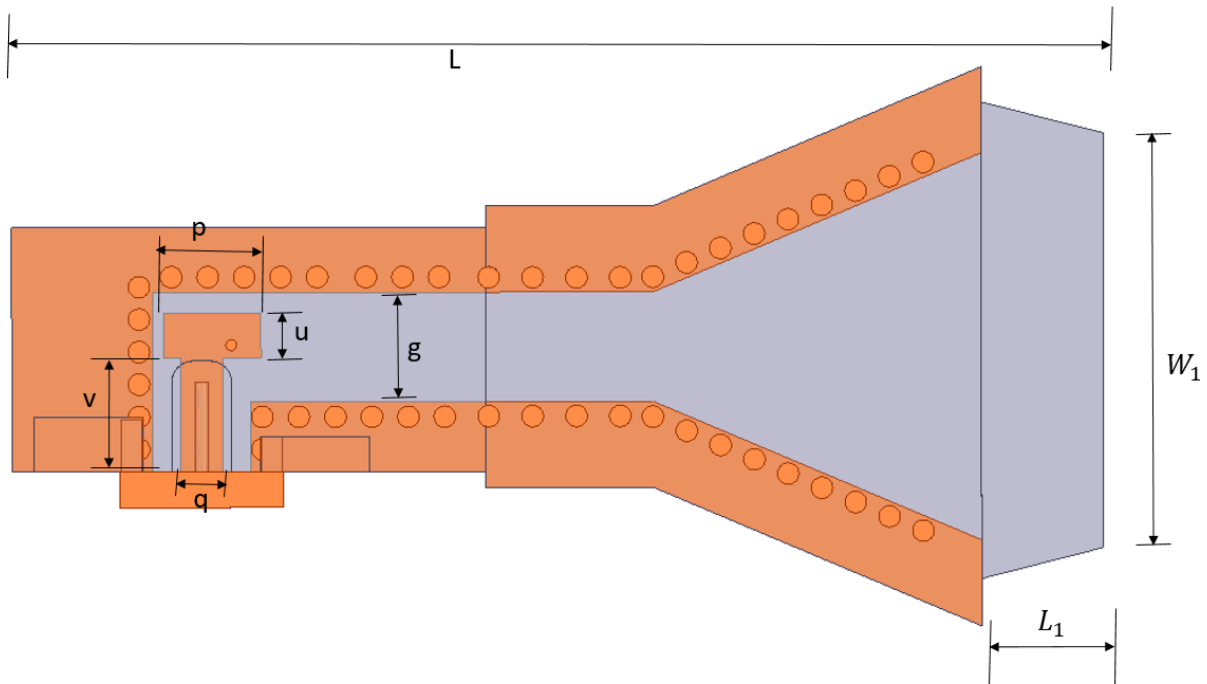


Figure 3.15 Cross Sectional view of LHCP type waveguide

$L=63.013\text{mm}$, $W_1=23.95\text{mm}$, $L_1=7.02\text{mm}$, $g= 6.3\text{mm}$, $u=2.55\text{mm}$, $v=6.57\text{mm}$, $p=5.61\text{mm}$, $q=2.45\text{mm}$, diameter of through holes= 1.25mm

Figure 3.15 shows the final design and dimensions of the LHCP type waveguide. It uses the SMA to SIEW Adaptor that has been discussed in Chapter 3.1. Horn section is placed after the adaptor

section and all the dimensions are shown in the Figure above. When the horn section is designed and placed the whole design is optimized again and the results have been evaluated. Distance between the through holes and the position of the post on the T-shaped copper strip, dimensions of the 'T' shaped copper strip are all the factors that are essential for the optimization. The length and width of the horn section and the dimensions of the dielectric load part are also taken into consideration during design process. The dielectric load contributes to a much lower reflection coefficient within the working frequency band. Dielectric load improves impedance matching by serving as the transition between the aperture and free space thereby the return loss is improved. After the optimization, reflections from the discontinuities can be cancelled out.

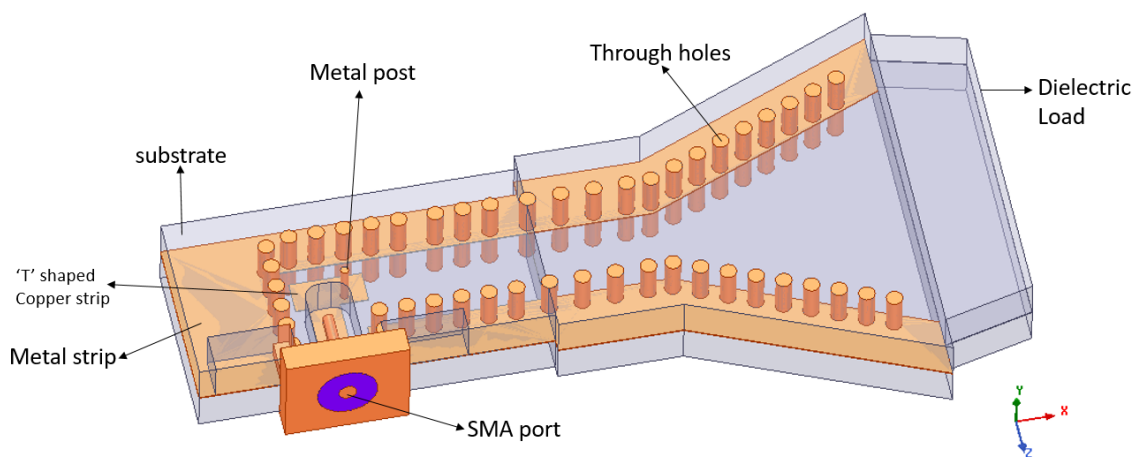


Figure 3.16 3D Geometry of Substrate Integrated LHCP waveguide

3.4.2 Simulated Results

After optimization using HFSS ANSYS, required results for obtaining LHCP wave have been achieved. Figure 3.17 shows the Reflection Parameters for the model and it can be seen that S_{11} parameters are below -15dB for the 14.4-15.5 GHz band and it reaches -40dB at 15.2GHz.

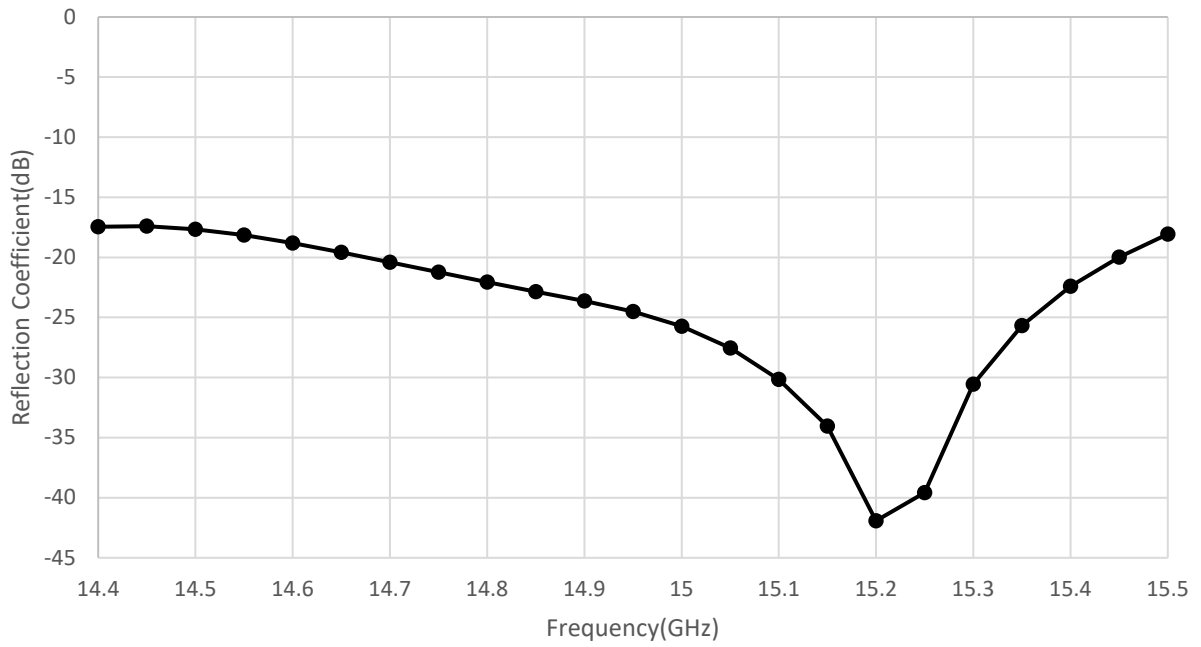


Figure 3.17 $|S_{11}|$ of Substrate Integrated LHCP Waveguide

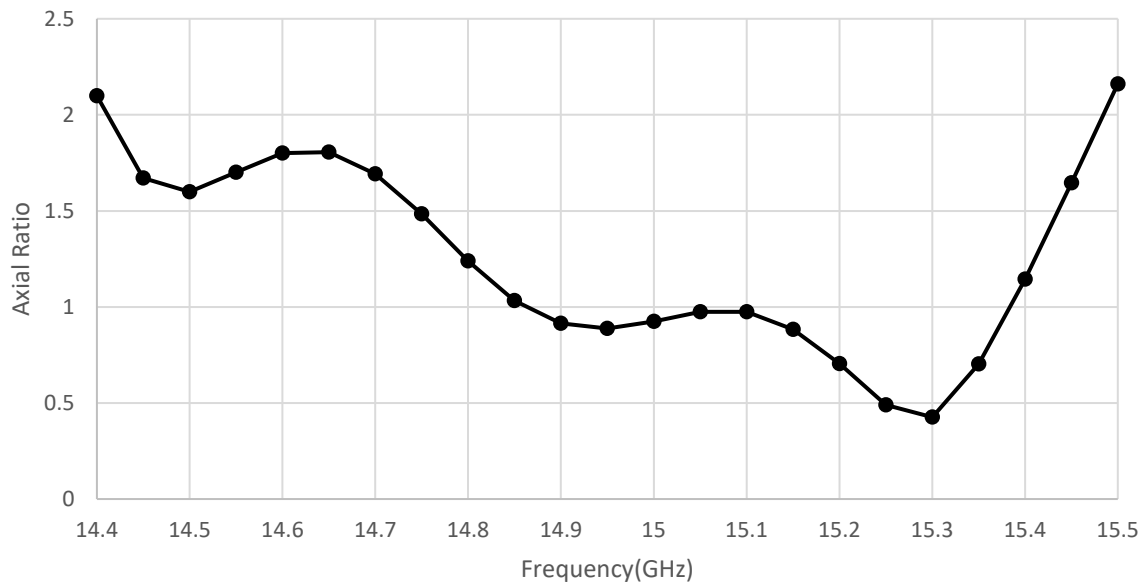


Figure 3.18 Axial Ratio Plot for Substrate Integrated LHCP Waveguide

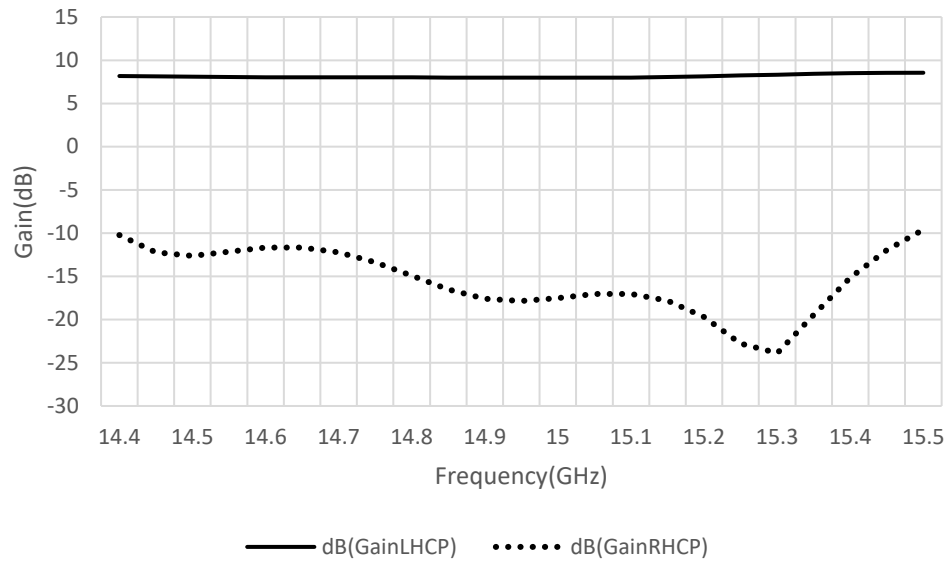


Figure 3.19 LHCP vs RHCP Gain Plot for Substrate Integrated LHCP Waveguide

To determine the circular polarization parameter, Axial Ratio is defined. Axial ratio is the ratio of orthogonal components of E-field. A circularly polarized field is made up of 2 orthogonal E-fields of equal magnitude and 90 degrees out of phase as discussed in Chapter 2.1. As both the components need to be of equal magnitude, it makes sense that the Axial Ratio needs to be 1 (0dB) for it to be perfectly circularly polarized wave. Axial ratio for ellipse should be greater than 1(0dB) as one of the component's magnitude is greater than the other. Similarly, for a linearly Polarized wave, the axial ratio is infinite. For example, if the Axial Ratio $< 3\text{dB}$ for ± 30 degrees from main beam indicates that deviation from circular polarization is less than 3dB over the angular range.

We can see from Figure 3.18 that the axial ratio $< 2\text{dB}$ over the 14.4-15.5 GHz band and 0.5dB at 15.3GHz and it is a good result for the wave to be circularly polarized.

Figure 3.19 shows the gain plot for the LHCP and RHCP waves for the model and it is clear that the gain for LHCP $> 7\text{dB}$ for 14.4-15.5 GHz band and whereas the gain for the RHCP $< -10\text{dB}$ over

14.4-15.5GHz band. This plot shows that the LHCP is dominating and hence the waveguide can be clearly said it is LHCP design without question.

3.5 Substrate Integrated RHCP Waveguide

3.5.1 Geometry of Substrate Integrated RHCP Waveguide

The geometry for the Substrate Integrated RHCP Waveguide is shown in the Figure 3.20, the polarizer design which has been stated in Chapter 3.2 is used and it is connected in between SMA to SIEW adapter and the horn section. Afterwards, the optimization is done using HFSS ANSYS and hence the lengths and widths of the septums are different from that of the design shown in Chapter 3.2. Similar to that in Figure 3.7, the first half of the polarizer section is symmetric to that of the other section for the sake of easy optimization.

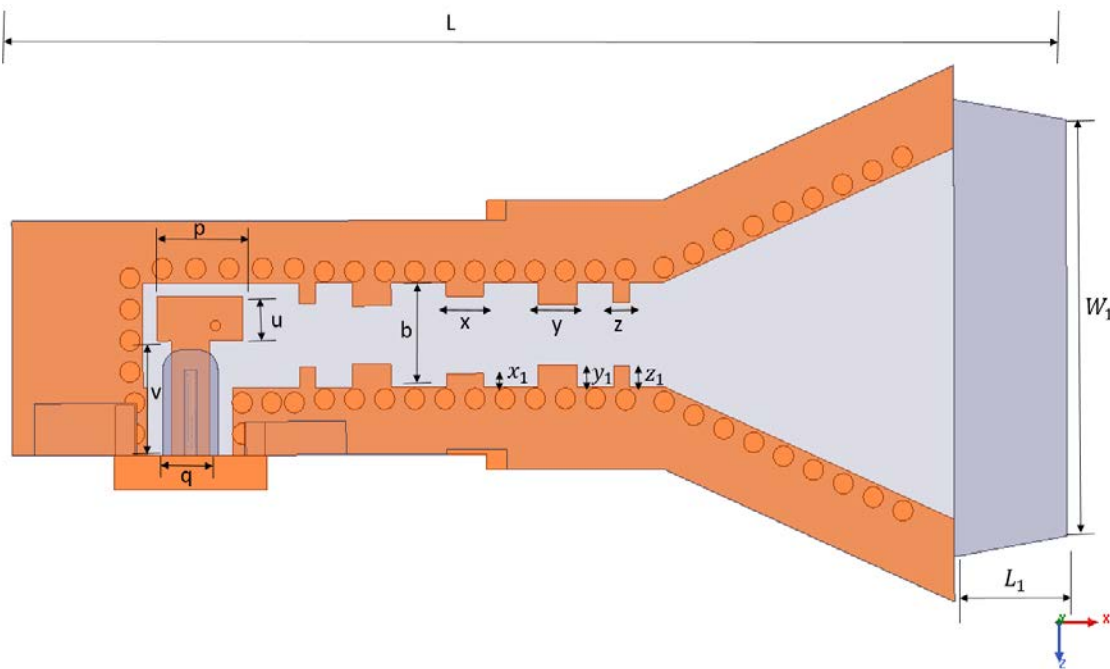


Figure 3.20 Cross Sectional view of RHCP type waveguide

$W_1=25.06\text{mm}$, $L_1=7.01\text{mm}$, $L= 65.7\text{mm}$, $p=5.32\text{mm}$, $u= 2.69\text{mm}$, $v=6.86\text{mm}$, $q=2.35\text{mm}$, $b= 6.3\text{mm}$, $x=2.31\text{mm}$, $y=2.42\text{mm}$, $z= 0.99\text{mm}$, $x_1=0.83\text{mm}$, $y_1=1.34\text{mm}$, $z_1=1.24\text{mm}$

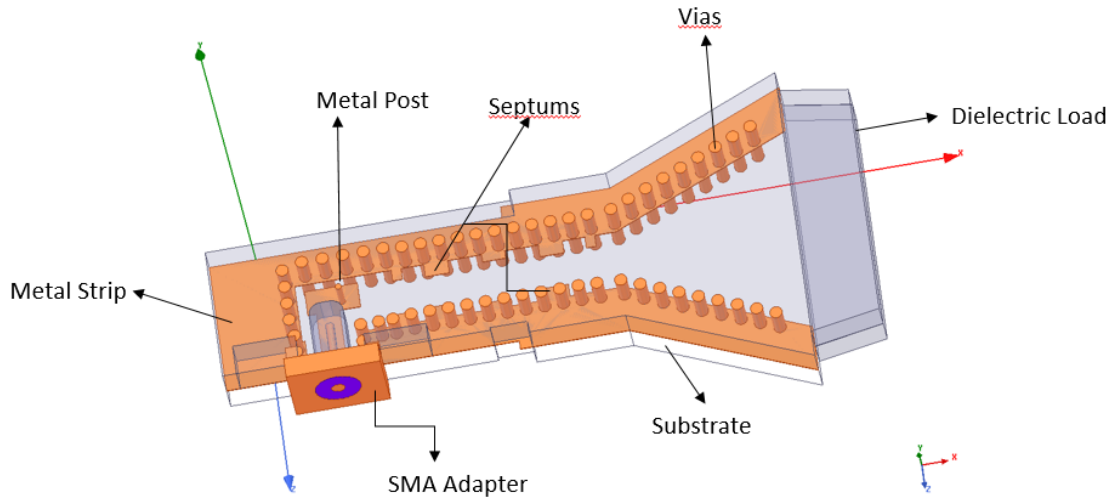


Figure 3.21 3D Geometry of Substrate Integrated RHCP Waveguide

After optimization, the dimensions of all the parameters are shown in Figure 3.20. The overall length ‘L’ is greater than that of the LHCP type Substrate Integrated Waveguide shown in Figure 3.15. As explained in Chapter 3.2, the phase delay of the horizontal wave is further increased with the presence of the septums extended on the copper strip in the middle. The positioning and the dimensions of these septums are optimized such that the required results are achieved. 3D model of the design is shown in Figure 3.21. In the next section, simulated results have been discussed.

3.5.2 Simulated Results

Figure 3.22 shows the reflection coefficient parameters plot for the Substrate Integrated RHCP Waveguide and we can see that $|S_{11}| < -15$ dB over the 14.4-15.4 GHz band. As we know that the reflection coefficient is supposed to be less than -10dB as the goal, this result is considered to be good for the model.

Figure 3.23 shows the axial ratio plot for the model and as we have discussed in Chapter 3.4.2, axial ratio is supposed to be 1 (0dB) for the wave to be perfectly circularly polarized. We can see from Figure 3.23 that the axial ratio < 2dB for 14.4-15.4 GHz band and less than 0.5dB at 14.4GHz and 15.2GHz which is as close to 0dB we can achieve using this design after optimization.

Figure 3.24 shows the RHCP vs LHCP plot for the model and we can read that the gain for RHCP curve is greater than 7dB whereas for LHCP, it is less than -15dB for 14.5-15.2 GHz band. These results confirm that RHCP type wave have been achieved using this Substrate Integrated RHCP waveguide design.

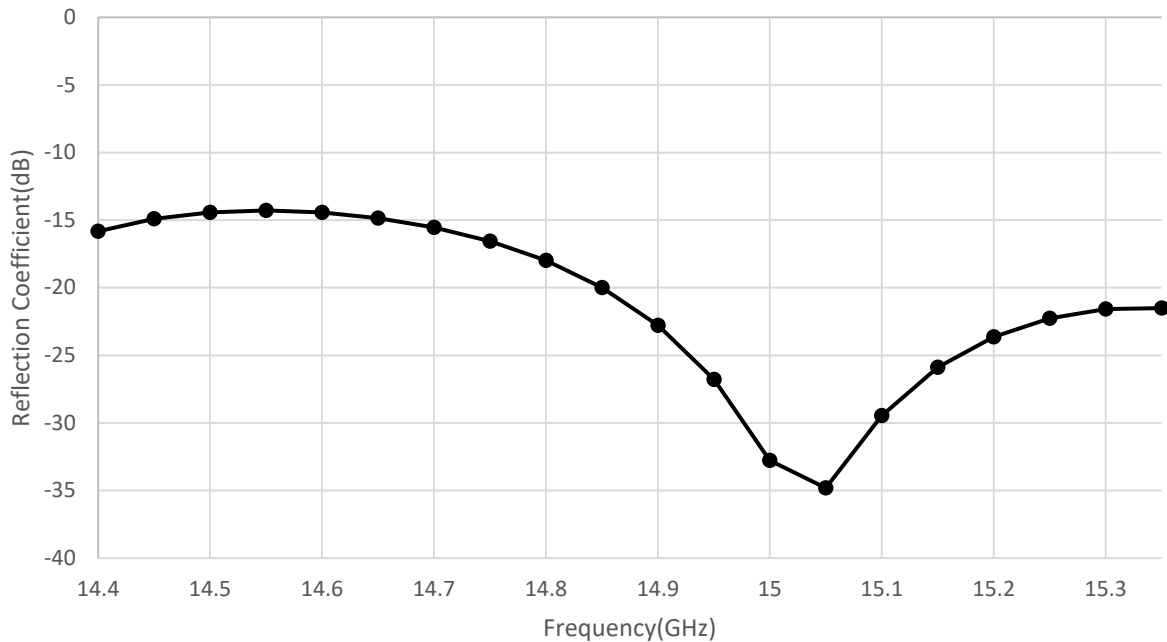


Figure 3.22 $|S_{11}|$ of Substrate Integrated RHCP Waveguide

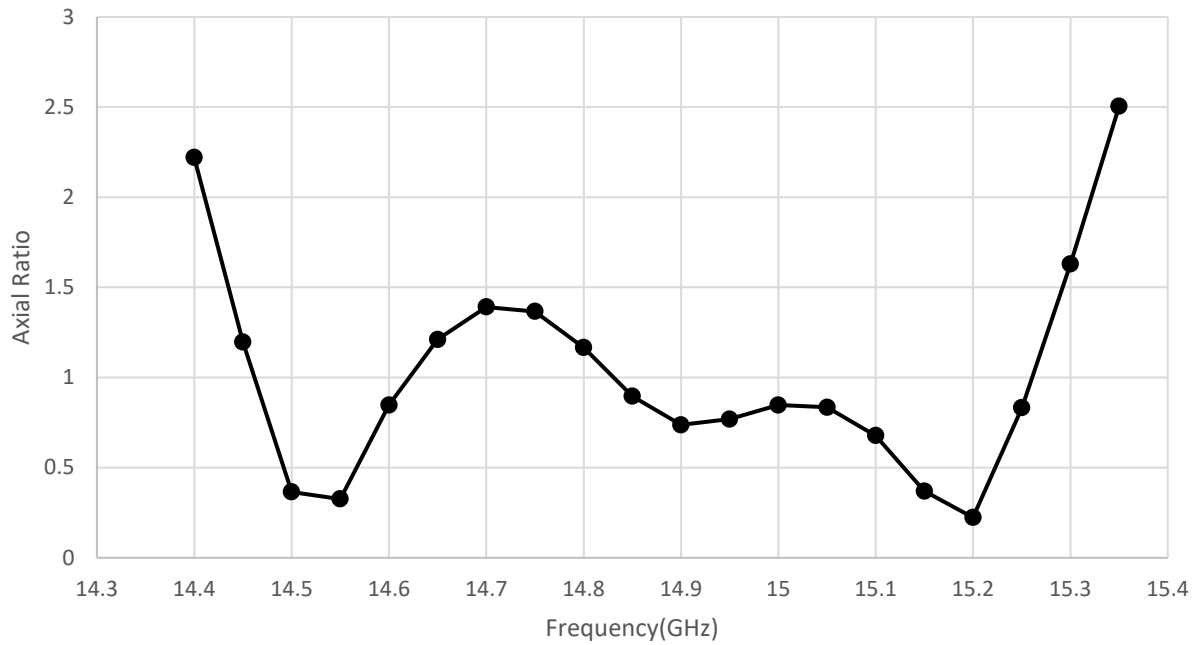


Figure 3.23 Axial Ratio Plot for Substrate Integrated RHCP Waveguide

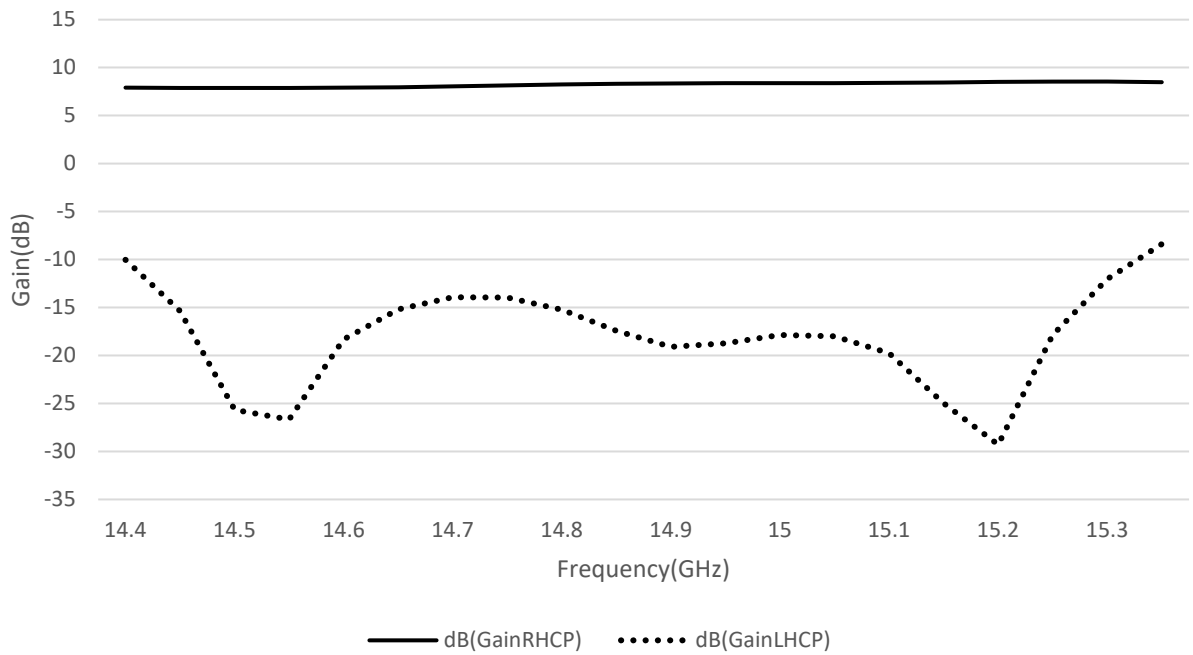


Figure 3.24 RHCP vs LHCP Gain Plot for Substrate Integrated RHCP Waveguide

4 Conclusion

In this paper, a novel substrate integrated circularly polarized Horn Antennas is proposed. Although, the conventional waveguide has better characteristics, it is inadequate for integrated circuits and micro level applications. Substrate Integrated Waveguide (SIW) technology and its applications which have been discussed cannot support E-plane type waveguide as wave cannot see the through holes on the Printed Circuit Board(PCB) and all the energy escapes. Hence, Substrate Integrated E-plane Waveguide technology concept have been used and this design is modeled using HFSS ANSYS emulation software. This waveguide structure is built by stacking two printed circuit boards and copper strip is sandwiched in between which supports E-field propagation. Concept of circular polarization has been widely used especially in the field of communications and hence this research has been focused on achieving circular polarization in a Substrate Integrated E-plane waveguide. This is done by placing of a metal post on the middle layer on the 'T' shaped copper strip which is electrically connected to SMA and extends until the top metal surface. The dimensions are optimized such that Phase delay of 90 degrees is introduced in E-plane along the length of propagation as it is important criteria for circular polarization.

The waveguide has been designed to work under frequency range of 14.4 to 15.4 GHz. Initial design has produced Left Hand Circularly Polarized Wave (LHCP), wherein the wave rotates in the clockwise direction. In the next design, a novel polarizer has been designed such that it introduces further phase delay to the E-field wave and hence Right Hand Circularly Polarized Wave (RHCP) has been achieved. For the LHCP design, simulation shows good return loss at 40dB and axial ratio is close to 0.4dB. For the RHCP design, simulation shows return loss at 35dB and axial ratio is close to 0.3dB. Conclusively, SIEW design to achieve circular polarization is potential and should be having many applications in the coming future.

5 References

- [1] D. M. Pozar, *Microwave Engineering*, John Wiley & Sons, Inc., 1990.
- [2] F. T. Ulaby, E. Michielssen and U. Ravaioli, *Fundamentals of Applied Electromagnetics*, NJ: Prentice Hall, 2001.
- [3] D. D. a. K. Wu, "Single-Substrate Integration Techniques for Planar circuits and Waveguide Filters," *IEEE Transactions on Microwave Theory and Techniques*, Feb, 2003.
- [4] Wu, D. Deslandes and a. K., "Accurate modeling, wave mechanisms, and design considerations of a substrate integrated waveguide," *IEEE Trans. Microw. Theory Techn.*, vol. 54, p. 2516–2526, Jun 2006.
- [5] K. Wu, D. Deslandes and Y. Cassivi, "The substrate integrated circuits - a new concept for high-frequency electronics and optoelectronics," *6th International Conference on Telecommunications in Modern Satellite, Cable and Broadcasting Service, 2003. TELSIKS 2003.*, 2003.
- [6] X. H. Wu, D. Huang and a. Q. Zhang, "Planar Substrate Integrated E-plane Waveguide (SIEW) circuits," *IEEE Transactions on Antennas and Propagation*, April 2017.
- [7] Wu, X.-P. Chen and a. K., "Substrate Integrated waveguide filters: Design techniques and structure innovations," *IEEE Microwave Magazine*, vol. 15, no. 6, Sep/Oct 2014.

-
- [8] A. Gopinath and P. R. Lal, "Substrate integrated waveguide based hybrid cavity filter for ku band applications," *2017 International Conference on Communication and Signal Processing (ICCSP)*, pp. 1563 - 1566, 2017.
- [9] H. J. Tang, W. Hong, J.-X. Chen, G. Q. Luo and a. K. Wu, "Development of millimeter wave planar diplexers based on complimentary characters of dual-mode substrate integrated waveguide filters with circular and elliptic cavities.," *IEEE Trans. Microw. Theory Techn.*, vol. 55, no. 4, pp. 776-782, Apr 2007.
- [10] D. Eom, J. Byun and H.-Y. Lee, "Multi-layer four-way out-of-phase power divider for substrate integrated waveguide applications," *2009 IEEE MTT-S International Microwave Symposium Digest*, pp. 477 - 480, 2009.
- [11] K. Song, S. Hu, M. Fan, Y. Zhu and Y. Fan, "Hybrid coaxial/substrate integrated waveguide eight-way power divider," *2015 IEEE MTT-S International Microwave Workshop Series on Advanced Materials and Processes for RF and THz Applications (IMWS-AMP)*, pp. 1 - 3, 2015.
- [12] M. N. Kumar and T. Shanmuganantham, "Substrate integrated waveguide tapered slot antenna for 57–64 GHz band applications," *2017 International Conference on Computer, Communication and Signal Processing (ICCCSP)*, pp. 1 - 6, 2017.
- [13] V. Arvind, R. Sowmiya, P. Vignesh, S. Kavin and M. Jayakumar, "Yagi slot antenna based on substrate integrated waveguide cavity for wider bandwidth applications," *2016 International Conference on Advanced Communication Control and Computing Technologies (ICACCCT)*, pp. 303 - 307, 2016.

-
- [14] M. Hedin, D. Huang, X. Wu and Q. Zhang, "Substrate Integrated E-plane Waveguide (SIEW) To Design E-plane and Dual Polarized Devices," *IEEE Transactions on Antennas and Propagation*, 2018.
- [15] Y.-C. Shih, "Design of waveguide E-plane filters with all-metal inserts," *IEEE Trans. Microw. Theory Techn*, Vols. MTT-32, pp. 695-704, Jul 1984.
- [16] V. Budimir and a. D.S, "Design of waveguide E-plane filters with all-metal inserts by equal ripple optimization," *IEEE Trans. Microw. Theory Techn.*, vol. 42, pp. 217-222, Feb 1994.
- [17] M. B. Manuilov and K. V. Kobrin, "Waveguide diplexer based on E-plane ridged sections and diaphragms," *2016 International Conference on Actual Problems of Electron Devices Engineering (APEDE)*, vol. 1, pp. 1-5, 2016.
- [18] N. Mohottige, B. Bukvic and D. Budimir, "Reconfigurable E-plane waveguide resonators for filter applications," *2014 44th European Microwave Conference*, pp. 299 - 302, 2014.
- [19] T. Su, C. Yu and M. Zhao, "W-band four-way E-plane waveguide power divider," 2016 IEEE MTT-S International Microwave Workshop Series on Advanced Materials and Processes for RF and THz Applications (IMWS-AMP), pp. 1-3, 2016.
- [20] W.-t. Zhang, L.-f. Ye, H.-y. Zhao and S.-l. Chai, "Design of waveguide E-plane hybrid metal insert filters for millimeter-wave application," *2010 International Conference on Wireless Communications & Signal Processing (WCSP)*, pp. 1-4, 2010.
- [21] Z. Gu, X. H. Wu and Q. Zhang, "Substrate-Integrated E-Plane Waveguide Horn Antenna and Antenna Array," *IEEE Transactions on Antennas and Propagation*, vol. 66, no. 5, pp. 2382 - 2391, May 2018.

-
- [22] D. Huang, X. H. Wu and Q. Zhang, "Concept of substrate integrated E-plane waveguide and waveguide filter," *2016 International Workshop on Antenna Technology (iWAT)*, 29 Feb.-2 March 2016.
- [23] G. Robb, "<https://antennatestlab.com>," Antenna Test Lab Co, [Online]. Available: <https://antennatestlab.com/wp-content/uploads/2017/09/CP-Explained-Without-Math.pdf>.
- [24] C. Zhu, T. Yamakawa, H. Zhao and H. Li, "All-Fiber Circular Polarization Filter Realized by Using Helical Long-Period Fiber Gratings," *IEEE Photonics Technology Letters*, vol. 30, no. 22, Nov.15, 15 2018.
- [25] J. K. G. e. al, "Gold helix photonic metamaterial as broadband circular polarizer," *Science*, vol. 325, no. 5947, pp. 1513-1515, Sep 2009.
- [26] J.-S. Row, W.-L. Liu and T.-R. Chen, "Circular Polarization and Polarization Reconfigurable Designs for Annular Slot Antennas," *IEEE Transactions on Antennas and Propagation*, vol. 60, no. 12, pp. 5998 - 6002, 2012.
- [27] Wu, F. Xu and a. K., "Guided wave and leakage characteristics of substrate integrated Waveguide," *IEEE Trans. Microw. Theory Techn.*, vol. 53, no. 1, p. 66–73, Jan 2005.
- [28] J. H. Ando and a. M., "Single-layer feed waveguide consisting of posts for plane TEM wave excitation in parallel plates," *IEEE Trans. Antenna Propagation*, vol. 46, no. 5, pp. 625-630, May 1998.